Available online at www.sciencedirect.com

SciVerse ScienceDirect

Geochimica et Cosmochimica Acta 77 (2012) 62–85

Geochimica et Cosmochimica Acta

www.elsevier.com/locate/gca

The impact of biotic/abiotic interfaces in mineral nutrient cycling: A study of soils of the Santa Cruz chronosequence, California

Art F. White *, Marjorie S. Schulz, Davison V. Vivit, Tomas D. Bullen, John Fitzpatrick

US Geological Survey, MS 420 345, Middlefield Rd., Menlo Park, CA 94025, USA

Received 23 July 2010; accepted in revised form 6 October 2011

Abstract

Biotic/abiotic interactions between soil mineral nutrients and annual grassland vegetation are characterized for five soils in a marine terrace chronosequence near Santa Cruz, California. A Mediterranean climate, with wet winters and dry summers, controls the annual cycle of plant growth and litter decomposition, resulting in net above-ground productivities of 280–600 g m^{-2} yr^{-1}. The biotic/abiotic (A/B) interface separates seasonally reversible nutrient gradients, reflecting biological cycling in the shallower soils, from downward chemical weathering gradients in the deeper soils. The A/B interface is pedologically defined by argillic clay horizons centered at soil depths of about one meter which intensify with soil age. Below these horizons, elevated solute Na/Ca, Mg/Ca and Sr/Ca ratios reflect plagioclase and smectite weathering along pore water flow paths. Above the A/B interface, lower cation ratios denote temporal variability due to seasonal plant nutrient uptake and litter leaching. Potassium and Ca exhibit no seasonal variability beneath the A/B interface, indicating closed nutrient cycling within the root zone, whereas Mg variability below the A/B interface denotes downward leakage resulting from higher inputs of marine aerosols and lower plant nutrient requirements.

The fraction of a mineral nutrient annually cycled through the plants, compared to that lost from pore water discharge, is defined their respective fluxes $F_{j,plants} = q_{j,plants}/(q_{j,plants} + q_{j,discharge})$ with average values for K and Ca ($F_{K,plants} = 0.99$; $F_{Ca,plants} = 0.93$) much higher than for Mg and Na ($F_{Mg,plants}$ 0.64; $F_{Na,plants} = 0.28$). The discrimination against Rb and Sr by plants is described by fractionation factors ($K_{Sr/Ca} = 0.86$; $K_{Rb/K} = 0.83$) which are used in Rayleigh fractionation-mixing calculations to fit seasonal patterns in solute K and Ca cycling. $K_{Rb/K}$ and $K_{^{24}Mg/^{22}Mg}$ values (derived from isotope data in the literature) fall within fractionation envelopes bounded by inputs from rainfall and mineral weathering. $K_{Sr/Ca}$ and $K_{^{44}Ca/^{40}Ca}$ fractionation factors fall outside these envelopes indicating that Ca nutrient cycling is closed to these external inputs. Small net positive K and Ca fluxes (6–14 mol m^{-2} yr^{-1}), based on annual mass balances, indicate that the soils are accumulating mineral nutrients, probably as a result of long-term environmental disequilibrium.
Published by Elsevier Ltd.

1. INTRODUCTION

Depths over which life-sustaining biotic and abiotic soil processes occur are surprisingly ill-defined (Richter and Markewitz, 1995). Studies in soil science and agronomy commonly equate soil depths and the corresponding cycling of vital mineral nutrients to zones of maximum biological activity associated with plant roots and the rhizosphere. In contrast, geochemical studies often equate soil depths to those of the regolith, produced by chemical and physical weathering with concurrent releases of mineral nutrients including K, Ca, Mg and Si. Ultimately these diverse approaches focus on reverse energy gradients; the thermodynamic instability of minerals, commonly formed under high temperature and pressure conditions in the earth's interior, producing weathering in the soil environment and the ability of plants, through photosynthetic reactions, to mobilize and physiologically concentrate these nutrients.

* Corresponding author. Tel.: +01 650 6526904.
E-mail address: afwhite@usgs.gov (A.F. White).

0016-7037/$ - see front matter Published by Elsevier Ltd.
doi:10.1016/j.gca.2011.10.029

The integration of these dual approaches, describing a complete soil system (*critical zone synthesis*; Brantley et al., 2006), requires defining the interfaces at which mineral nutrient fluxes, reflecting abiotic processes and gradients in deeper soils, become modified and dominated by biogenic processes and cycling in shallower soils. In discussing such biotic/abiotic interfaces, it is recognized that diminished biologic processes, principally microbial activity, certainly occur at significant depths below this interface (Buss et al., 2005), while abiotic inputs from chemical weathering and precipitation, occur above this interface (White et al., 2008a,b).

Most studies on abiotic/biotic interactions focus on forested watersheds, particularly on environmental impacts of acid precipitation and the role of weathering as a neutralizing agent and a source for base cation resupply (Huntington, 2000; Driscoll et al., 2005). Far fewer efforts focus on the coupling of weathering and mineral nutrient cycling in grasslands, even though they cover 35% of the earth's land mass and have high annual productivities compared to other ecosystems (Kelly et al., 1998; Christian and Wilson, 1999; Gibson, 2009). Grasslands commonly encompass areas of lower topography and drier climates than forest ecosystems, making integrated watershed approaches less productive. However, the temporal and spatial scales associated with grassland/soil processes are small and relatively well-defined, with shallow rooting depths and high annual biomass turnover rates. Both scales emphasize the importance of nutrient inputs from precipitation and chemical weathering and subsequent cycling between the soil and biomass.

The present study describes mineral nutrient sources and cycling in a coastal prairie grassland ecosystem established on a soil chronosequence consisting of uplifted coastal terraces along the central Pacific Coast of California. In addition to characterizing soil and biomass reservoirs, mineral nutrient pathways are differentiated in terms of fluxes across the biotic/abiotic interface. Also addressed are the complexities associated with defining open and closed soil nutrient cycling and the extent to which nutrient imbalances reflect long-term environmental disequilibrium. The mineral nutrients discussed in this paper are limited to cations contained in soil minerals, mobilized during chemical weathering and subsequently utilized by plants. By this definition, the major mineral nutrients are K, Ca, Mg and to a lesser extent, Na. Strontium and Rb are also included as they serve as useful nutrient tracers. Silica, an additional important mineral nutrient, will be discussed in a separate paper.

This study describes important macroscale nutrient distributions and fluxes between plants and soils but not the complex microscopic biological pathways controlling nutrient uptake and utilization by the plants (Marschner, 1995; Maathius, 2009). The paper presents new data on plant and pore water compositions, as well as interpreting these results using previously published work on the Santa Cruz sites including soil mineralogy and long-term weathering rates (White et al., 2008a), Ca isotope distributions (Bullen et al., 2004), pore water hydrology and solute weathering (White et al., 2009), reactive transport processes (Maher et al., 2009), microbiology (Moore et al., 2009), pedogenic Fe formation (Schulz et al., 2010) and Mg isotope distributions (Tipper et al., 2010).

2. SITE DESCRIPTION AND METHODS

The Santa Cruz study sites are adjacent to the Pacific Ocean, northwest of the city of Santa Cruz, and situated approximately 50 km SW of San Francisco (Fig. 1). Yearly mean temperature and rainfall for the city of Santa Cruz are 13.4 °C and 0.85 m (White et al., 2008a). The sites comprise a temperate California coastal-prairie ecosystem dominated by non-native annual grasses and a lower abundance of perennial forbes, most of which have been introduced to California over the last two hundred years (Stromberg et al., 2007). The preservation of the remaining native species in these coastal environments is an important environmental management issue (Gibson, 2009).

The soils comprise a chronosequence formed on a series of uplifted terraces underlain at relatively shallow depths by reworked beach sediments primarily derived from granitic plutons in the adjacent Santa Cruz Mountains. Soils in the chronosequence, classified as loamy molisols (Aniku and Singer, 1990) have been age-dated using ^{10}Be (Perg et al., 2001) and sequentially defined in this and previously papers as the SCT 1 (65 ka), SCT 2 (90 ka), SCT 3 (137 ka), SCT 4 (194 ka) and SCT 5 (226 ka) soils. The soils contain secondary kaolinite and Fe oxides which become increasing concentrated in argillic horizons in older soils at depths of 0.5–1.5 m. Details of the soil mineralogy and chemical compositions are contained in White et al. (2008a).

Soil samples, obtained by hand augering to depths of up to 15 m, are described in terms of chemistry, mineralogy and cation exchange characteristics by White et al. (2008a,b, 2009). Soil pore water was measured gravimetrically on samples weighed before and after heating to 80 °C for 24 h. Rain samples were collected using plastic funnels connected to one liter bottles. No attempt was made to sample aerosols during the dry summer months. Pore waters from the generally unsaturated soils were extracted by nested ceramic-tipped suction water samplers evacuated to 80 cbars. During dry summers, moisture tensions in the shallower soils commonly exceeded those imposed by the suction samplers and pore waters were not obtained. Precipitation and pore waters were analyzed by ICP-MS and ion chromatography. Accepted results, replicated against reference standards, had errors of $<5\%$.

Plant species at the SCT 2 and SCT 3 sites, located within Wilder State Park, were described in detail by park biologists. Cursory surveys of the other sites found similar vegetation types. Above-ground vegetation at all sites was collected at monthly intervals over a yearly growth/dieback cycle (October 2002 to November 2003). Standing grass was cut to ground level using garden shears from adjacent one square meter sampling grids. Fallen litter, in various stages of decay, was collected from the soil surface by hand. Significant efforts were made to exclude mineral soils during sampling. Root distributions were estimated visually in hand-dug soil pits and described by a semi-quantitative

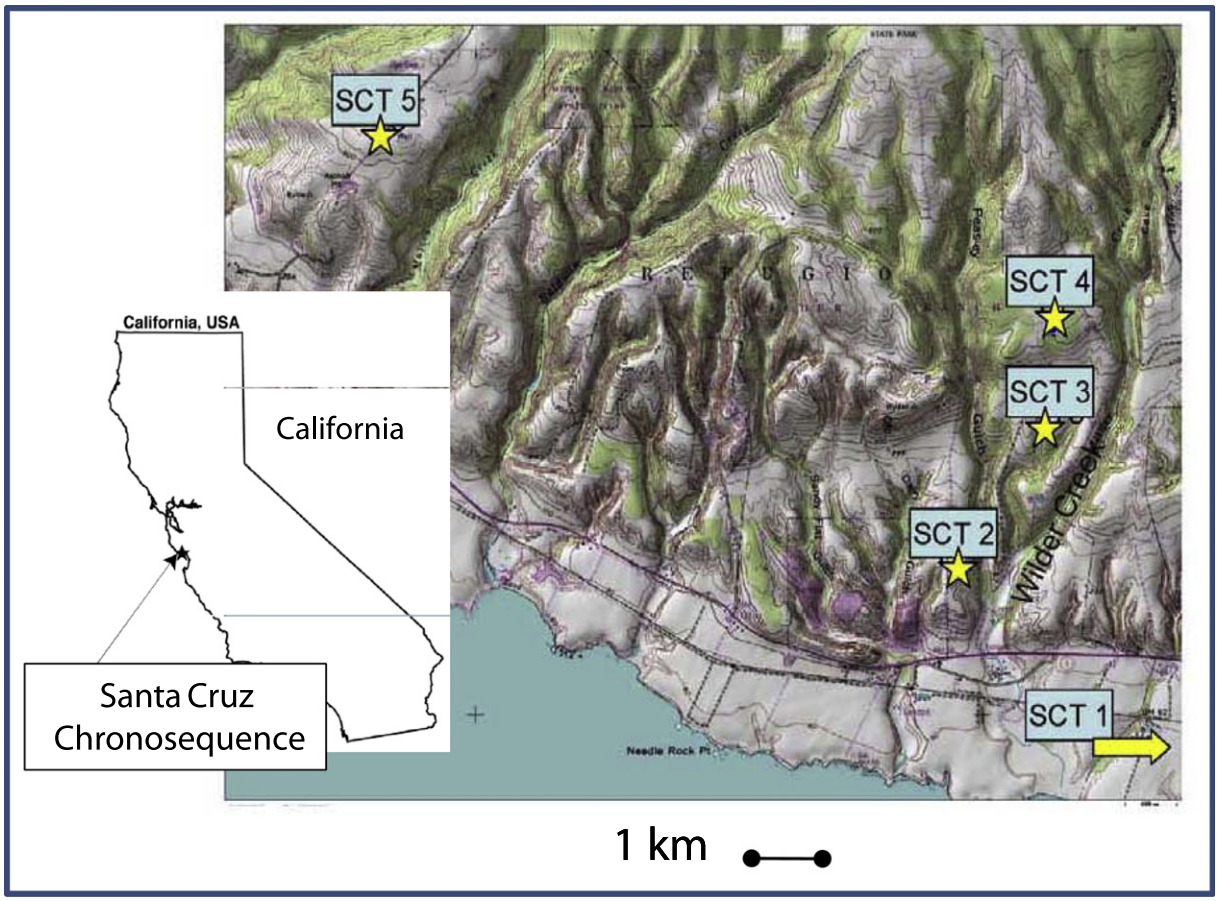

Fig. 1. Location of the Santa Cruz soil sites (the SCT 1 site is approximately 5 km east of map area).

root index (Pinney et al., 2002) using observed root size (very fine = 1 to course = 4) and frequency (rare = 10 to common = 30). No attempt was made to collect root samples.

Vegetation samples were stored in the laboratory at room temperature in large paper bags. Dry weights were established after successive monthly measurements varied by less than 5%. Vegetation samples were ground and homogenized using a commercial kitchen blender. Analyses of major elements were performed at the Agricultural Sciences Department at Oregon State University using ICP-AES and CNS. Standard errors for blind replicates were <5%. Selected vegetation samples were analyzed for Rb and Sr at the USGS using ICPMS after dry ashing and digestion with nitric acid (Giron, 1973).

3. RESULTS

A complete plant list for the SCT 2 and SCT 3 sites are contained in Appendix A. Total above-ground biomass and corresponding major and trace element compositions for five sites, sampled from the fall of 2002 through the fall of 2003, are contained in Appendix B. Selective compositions of rain and pore waters from soil depths of 0.15 and 1.2 m at the SCT 2 and SCT 5 sites are listed in Appendix C. The tables and plots presented in this paper do not always contain data inclusive for all five soil sites. Unless otherwise note, reported results are consistent with available data for the other sites.

3.1. Grassland biomass

The above-ground dry biomasses ($g\,m^{-2}$) for the five sites measured during the 2002–2003 growth cycle are plotted in Fig. 2 (data in Appendix B). A strong correlation exists between seasonal wet and dry periods and cycles of plant growth and dieback (Fig. 2a). Low biomass, collected during the initial fall sampling in October, 2002, consisted of standing dead grass and dry litter, reflecting the lack of significant precipitation since the preceding late spring (Fig. 2b–f). The first subsequent rain occurred shortly afterwards in early November of 2002 (vertical solid lines on the left of Fig. 2b–f).

Significant new plant growth, responding to the onset of increased solar radiation and temperature, did not occur until later in the winter. Biomass subsequently increased throughout the spring corresponding to periods of maximum plant growth. After the last rain in May of 2003 (dashed vertical lines in Fig. 2b–f), soil moisture gradually exceeded the wilting potential of the vegetation. Plant growth ceased in the early summer and the above-ground biomass declined until the onset of the next rainy season

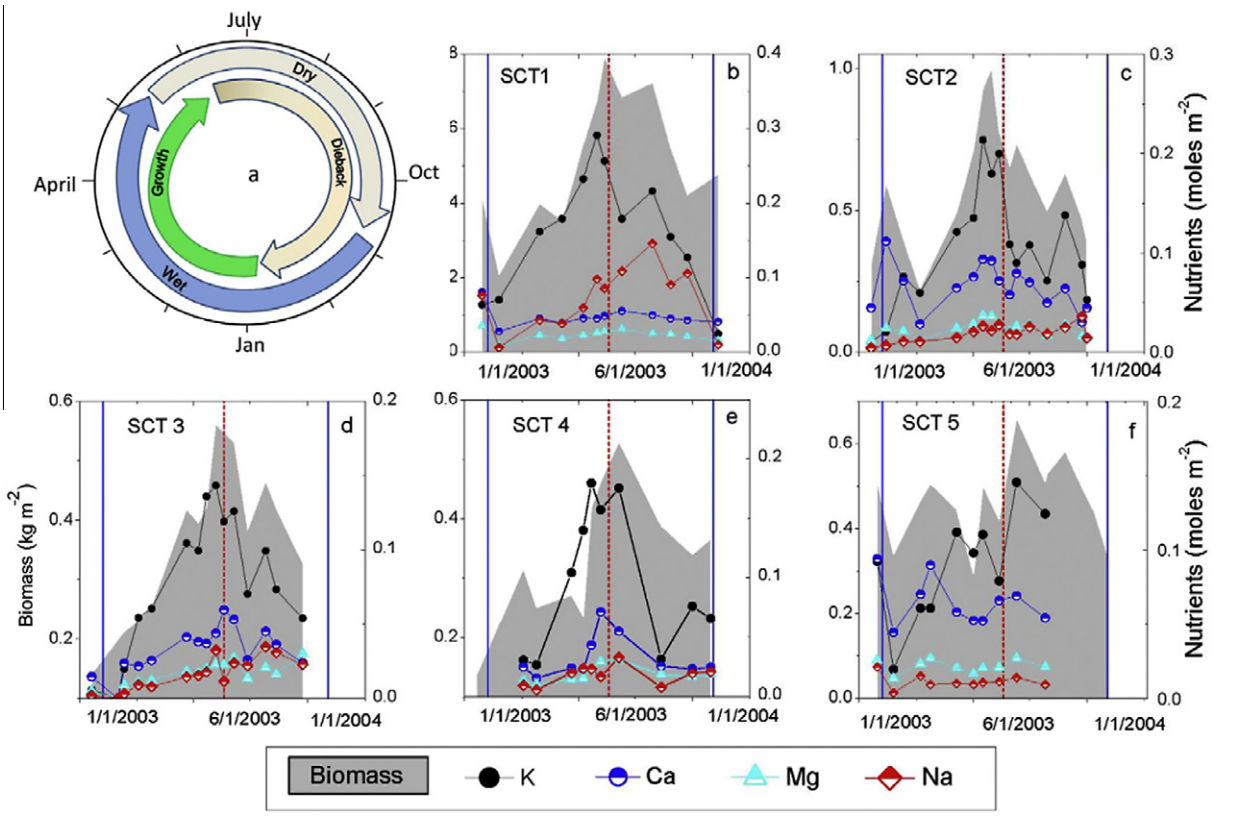

Fig. 2. Seasonal variabilities in grassland vegetation. (a) Schematic showing cyclic relationship between rainfall (outer circle) and plant growth (inner circle). (b–f) Annual variations in biomass (kg m^{-2}) and mineral nutrients (moles m^{-2}). Vertical solid lines correspond to first major rainfalls in the fall of 2002 and 2003 and vertical dashed line to last major rainfall in the spring of 2003.

in October of 2003 (vertical solid line on the right side of Fig. 2b–f). Grass litter decomposition studies performed elsewhere in the Santa Cruz Mountains indicate photo-degradation during the summer months accounts for about 10% of biomass loss and microbially-driven decomposition at the beginning of the subsequent rainy season accounts for up to 50% biomass loss (Henry et al., 2008).

The annual net primarily plant productivity ANNP (Scurlock et al., 2002) is the difference between the maximum above-ground biomass measured in the spring and the minimum biomass measured in the fall (Appendix B). ANNPs listed in Table 1 are higher for the SCT 1 and SCT 2 soils (585–600 g m^{-2}) than the SCT 3, SCT 4 and SCT 5 soils (280–350 g m^{-2}). The range in these values is generally lower than those reported for other temperate grasslands (750 g m^{-2} yr^{-1}; Gibson, 2009). Grassland ANPPs commonly increase with increasing precipitation (Heister-White et al., 2008), a correlation not observed at Santa Cruz. Due orographic effects, rainfall increases by about a factor of two from the younger to the older terraces (White et al., 2009). Higher ANPPs for the SCT 1 and SCT 2 sites, closer to the ocean (Fig. 1), may reflect foggier conditions which persist through the late spring and summer. Nutrient availability may also be lower in the older more weathered soils, as demonstrated for other chronosequences (Chadwick et al., 1999).

Table 1
Annual net primary productivity ANPP (g m^{-2}), and plant uptake of major elements (mmoles m^{-2} yr^{-1}).

	SCT 1	SCT 2	SCT 3	SCT 4	SCT 5
ANPP	585	600	350	280	325
C	21,050	21,950	12,600	10,650	13,300
N	431	254	192	176	252
K	249	104	124	149	126
Ca	21	20	20	40	25
Mg	20	15	14	21	14
Na	80	11	29	27	10
Si	165	111	83	43	62
S	18	17	13	11	12

Root distributions in the SCT 2, 3 and 5 soils are plotted in Fig. 3a based on the semi-quantitative abundance index (Pinney et al., 2002). Root abundances are greatest near the soil surface and decrease with increasing depth. These distributions agree with root development models describing linear or exponential density decreases with depth (Gregory, 2006) and with the range of rooting depths reported for grassland species found on the Santa Cruz soils (Appendix A). As expected, root distributions generally correlate with soil organic carbon content (Fig. 3b; Moore et al., 2009). Above and below-ground biomasses are compared by root-to-shoot ratios (R/S) which commonly approach unity for annual grasses whose growth is limited to wet

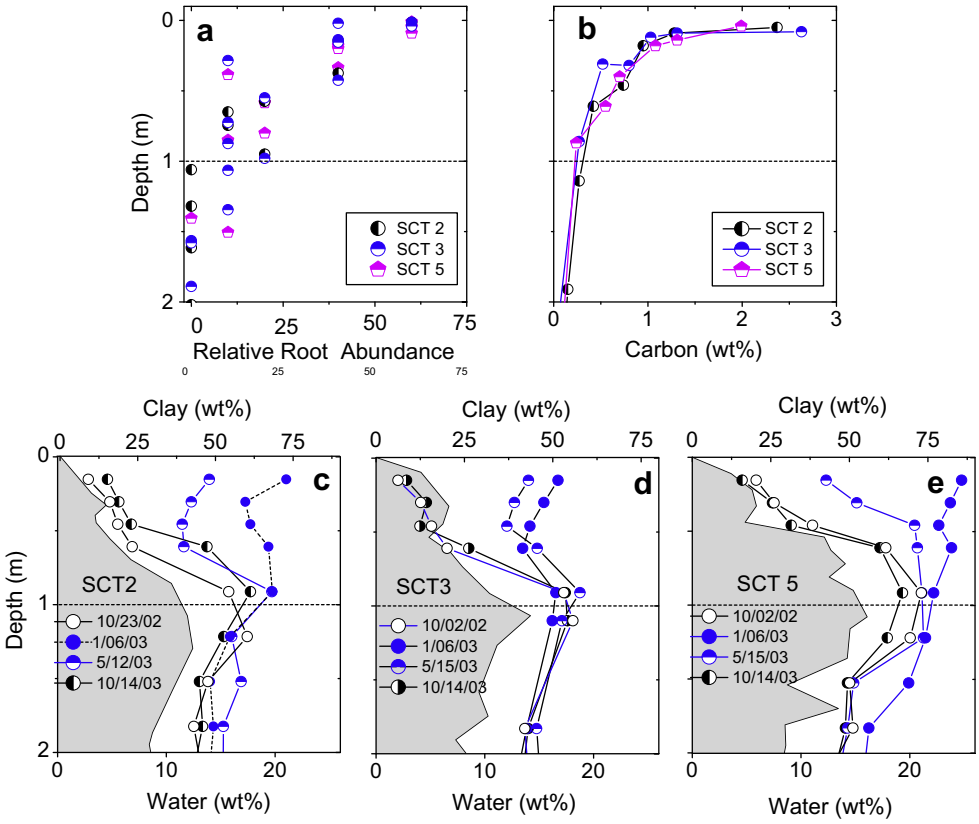

Fig. 3. Below-ground soil characteristics. (a) Root distributions based abundance index (after Pinney et al., 2002). (b) Soil organic carbon distributions (after (Moore et al., 2009). (c–e) Pore water distributions sampled during seasonal plant growth and dieback (partial data listing in Appendix C). The horizontal dashed lines correspond to the approximate depth of A/B interface and maximum clay contents as indicated by the shaded areas (clay data from White et al. (2008a,b)).

conditions (Monaco et al., 2003; Snyman, 2009). For the annual Santa Cruz grasses, both shoots and roots are subjected to seasonal growth and decay, potentially doubling annual biomass cycling (ANNPs in Table 1).

3.2. Plant mineral nutrient concentrations and fluxes

Elemental compositions in vegetation sampled during the 2002–2003 growth cycle are contained in Appendix B and normalized to biomass and land surface (moles m^{-2}) in Fig. 2b–f. Potassium is the dominant mineral cation followed by Ca and Mg. K is incorporated into large number of plant enzymes. Calcium forms oxalates and pectates critical to cell wall stabilization. Magnesium is associated with chlorophyll production and protein synthesis (Marschner, 1995). Elemental concentrations in the Santa Cruz vegetation (Appendix B) are comparable to averages for other temperate grasslands (Whitehead, 2000).

Changes in total amounts of Ca and Mg are proportional to changes in biomass during the growth/dieback cycle. Potassium peaks earlier than the biomass in the late spring and is selectively lost during dieback and litter decay (Appendix B and Fig. 2b–f). Sodium exhibits the lowest correlation with biomass, continually increasing throughout much of the year. Most plants (except halophytes) discriminate against Na which is generally more abundant in soil pore waters than other elements, especially K. Sodium probably reflects the accumulation of sea salt aerosols on the plant surfaces, as suggested by anomalously high Na for vegetation at SCT 1 site which is closest to the ocean (Fig. 1). In coastal environments, Na contained in sea spray commonly interferes with plant metabolism (Ashraf et al., 1989).

3.3. Seasonal water availability

Soil moisture profiles correlate with seasonal rainfall patterns (Fig 2a and Fig. 3c–e; a partial listing of water contents is contained in Appendix C). Soil waters sampled in October of 2002 and 2003 are from the driest soils (<5 wt.% water). Soil tensions measured during those times exceed the wilting potential of the annual grasses (White et al., 2009). In January of 2002 and 2003, shallow soils exceed 20 wt.% water, reflecting inputs from large winter storms and low transpiration rates before the start of the growing season. Diminished moisture contents later in May of 2003 correspond to decreasing inputs from late spring rains, coupled with high transpiration rates associated with maximum plant growth. Seasonal moisture variabilities diminish with increasing soil depths, becoming relatively constant below one meter (Fig. 3c–e). Except for the wettest period in January, maximum soil water also

occured at about one meter, corresponding to the soil horizons with the highest clay contents.

3.4. Solute cation compositions and trends

Pore water cations sampled in the SCT 2 and SCT 5 soils between January 2002 and June 2004 are plotted in Fig. 4 (partial data tabulation in Appendix C). Elemental variabilities are generally greatest in the shallowest soils and decline with increasing soil depths. The most dilute pore waters are comparable to concentrations found in precipitation (rainfall data in Appendix C). Average cation compositions (interconnected lines in Fig. 4) are biased toward wet season samples due to the inability to extract water from the shallower soils during the drier summer months.

Average solute Na consistently increases with soil depth. Magnesium increases down to the argillic horizon (horizontal lines in Fig. 4) and then decreases in the deeper soils. Calcium and K are highest in the shallowest soils and decline to low concentrations below the argillic horizon. These profiles fit the general observation that mineral nutrients used more extensively by plants and limit their growth, such as K and Ca, have shallower distributions than those which are less limiting, such as Mg and Na (Jobbagy and Jackson, 2001). Strontium and Rb, while present in much lower concentrations, generally follow the respective trends for Ca and K (Fig. 4).

Relative cation abundances are significantly different above and below the argillic horizon as expressed as cation ratios in pore waters extracted from suction water samples nested at or above 0.60 m and at or below 1.2 m (open and closed circles in Fig. 5). Calcium exhibits the widest range in solute concentrations and is selected as the common variable in the plots (horizontal axes in Fig. 5). Evapotranspiration (ET) accounts for up to 85% of soil moisture loss (White et al., 2009) and its effect on pore water concentrations is shown by the upward extrapolation of average volume-weighted rain compositions (solid diagonal lines with slopes of unity in Fig. 5).

Proportions of Sr, Mg and Na, relative to Ca, are generally higher in the deeper pore waters at or below 1.2 m and plot along linear trends above the ET lines (diagonal dashed lines in Fig. 5). The variation between individual samples along these trends is principally depth-related. Higher cation concentrations generally correspond to deeper pore waters that reflect increased weathering of

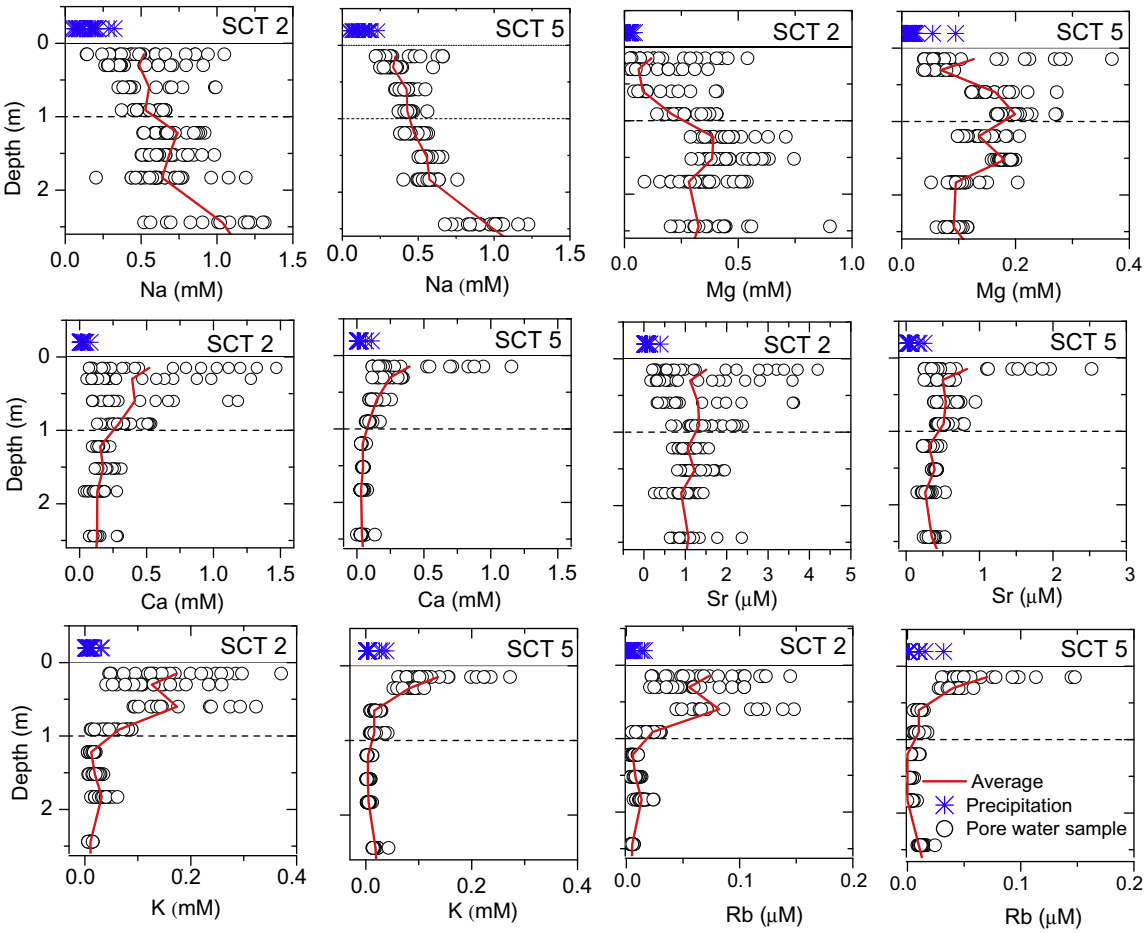

Fig. 4. Compositions of pore water (open circles) and rainfall (stars) at the SCT 2 and 5 sites measured from 2002 to 2004 (partial data listing in Appendix C). Solid lines are averages of pore water data from a specific depth. The horizontal dashed lines correspond to the approximate depth of maximum clay contents (Fig. 3c–e) and the A/B interface.

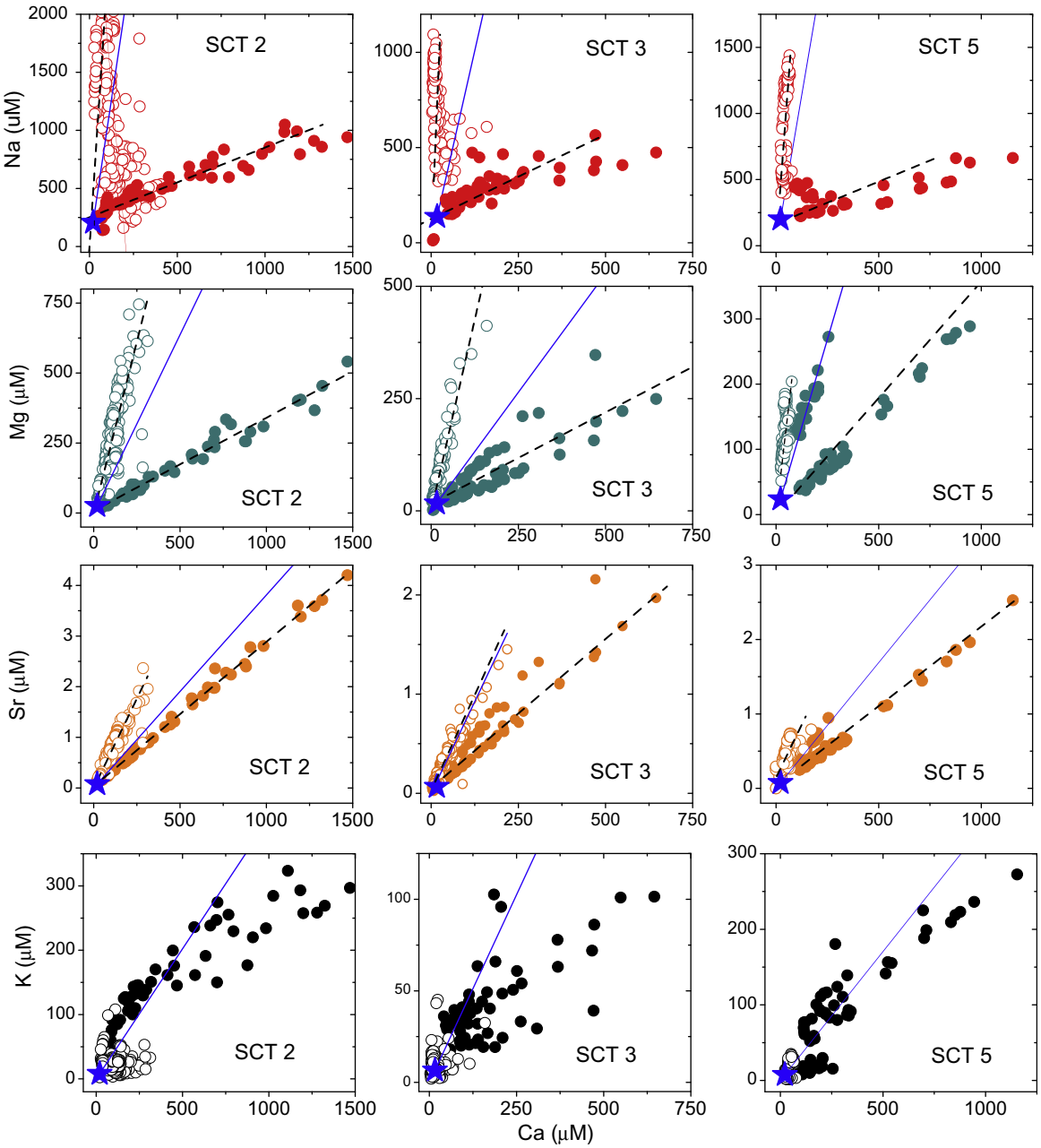

Fig. 5. Cation ratios in soil pore waters. Closed circles are pore waters sampled at ⩽0.6 m depth and open circles are for pore waters ⩾1.2 m depth (partial listing of data in Appendix C). Depths bracket maximum clay contents and the A/B interface at one meter (Fig. 3c–e). Evapotranspiration trends (solid lines) are extrapolated from average precipitation concentrations (stars). Slopes to the linear regression fits to pore waters (dashed lines; *K* excluded) are reported as elemental ratios in Table 2 and used to calculate similarity factors $S_{i,j}$ (Eq. (1)).

plagioclase and smectite (White et al., 2008a). Proportions of Sr, Mg and Na, relative to Ca, are lower in pore waters sampled at or above 0.6 m and generally plot along trends below the ET lines (Fig. 5). These lower ratios reflect greater amounts of Ca cycled through the vegetation. Cation abundances at these depths primarily reflect seasonal variabilities, with the lowest concentrations occurring during active plant growth and the highest concentrations during plant dieback.

The general linearity in these shallow pore water trends indicates that uptake and subsequent release of Ca, Sr, Mg, and Na by the vegetation must occur in relatively constant proportions in spite of the different roles these elements play in biological processes. In contrast, non-linearity in proportions of K relative to Ca (Fig. 5) suggests divergent behavior during plant uptake and liter decomposition. Potassium and Ca have very different delivery mechanisms to the plant root; K requires diffusion transfer involving metabolic processes whereas Ca delivery is by passive mass transport (Marschner, 1995). During litter decay, K is associated with the labile organic fraction while Ca is contained in less soluble oxalates and pectates.

The degree to which abiotic and biotic cation trends converge (dashed diagonal lines in Fig. 5) is related to their chemical similarity. Elements of comparable affinities behave similarly in both abiotic and biotic processes and elements of differing affinities behave dissimilarly. Some studies find a strong correlation between cation radius and charge and their correspondingly behaviors in soils and plants (Tyler, 2004). The extent of convergence of the linear trends in Fig 5 is quantified by a similarity factor $S_{i,j}$ where i and j are individual cations

$$S_{i,j} = \frac{[C_i/C_j]_{biotic}}{[C_i/C_j]_{abiotic}} \quad (1)$$

Values approaching of $S_{i,j} = 1$ indicate very similar cation behavior under both abiotic and biotic conditions while values approaching $S_{i,j} = 0$ indicate dissimilar behavior. Regression fits (r values are generally >0.85) determine the slopes of the linear pore water trends and the corresponding biotic and abiotic cation ratios (Table 2). Calcium and Sr are the most similar (average $S_{Sr,Ca} = 0.36$), Mg and Ca are moderately similar ($S_{Mg/Ca} = 0.13$) and Na and Ca are the most different ($S_{Na,Ca} = 0.04$).

3.5. Sr/Ca and Rb/K distributions and fractionation factors

Ratios of trace and major elements with high degrees of chemical similarity, e.g., $S_{Sr/Ca}$ (Table 2) are used to investigate abiotic and biotic processes in soils (Drobner and Tayler, 1998; Blum et al., 2000; Bullen and Bailey, 2005). While the behaviors of major mineral nutrients are generally well understood, the roles of the corresponding trace elements are generally ill-defined. An important issue is whether or not they simply substitute for their major element counterparts or else play specific roles in plant physiologic processes (Marschner, 1995).

Plants concentrate or exclude Sr relative Ca depending on the species, the parts of the plant considered, i.e., roots, stems and leaves, and the external environment, i.e., solutes, exchangeable cations or bulk soils compositions (Poszwa et al., 2000; Dasch et al., 2006). Representative Sr and Ca data are listed in Appendix C with distributions in the SCT 5 soil plotted in Fig 6a. The shallowest pore waters (0.15 m) have an average ratio (Sr/Ca = 0.0029) that is only slightly higher than grasses (Sr/Ca = 0.0024) but is significantly lower than precipitation (Sr/Ca = 0.0047). Solute Sr/Ca ratios increase with soil depth across the argillic horizon (horizontal lines in Fig. 6) and in the deeper soils are similar to those expected for plagioclase weathering (Ca/Sr = 0.0102; White et al., 2009).

Rubidium is used as a tracer in plant nutrient studies with uptake dependent on soil acidity, exchange capacity and K availability (Drobner and Taylor, 1998). Rb/K ratios are used in estimating contributions of biogenic K to watersheds and river systems (Chauduri et al., 2007; Peltola et al., 2008). Representative Rb and K data are contained in Appendix C with distributions in the SCT 5 soil plotted in Fig 6b. The average K/Rb ratio in the shallowest pore water (0.00049 at 0.15 m) is slightly higher than average grass (Rb/K = 0.00042) which is similar to ratios reported for other plants (Conner and Shacklette, 1975; Peltola et al., 2008). Shallow pore waters and grass Rb/K ratios are higher than precipitation at the SCT 5 site (Rb/K = 0.00027; selected data listed in Appendix C). Pore water Rb/K ratios exhibit increases with depth (Fig. 6b), attributable to Rb/K = 0.00075 in K-feldspar (Fig. 6b; data from White et al., 2008a).

Elemental distributions between plants and the soil environment are defined by a fractionation factor $K_{i,j}$ in which the ratio of concentrations of the trace component C_i and major component C_j in plants is divided by the corresponding ratio in the soil

$$K_{i,j} = \frac{[C_i/C_j]_{plant}}{[C_i/C_j]_{soil}} \quad (2)$$

$K_{i,j} > 1$ indicates preferential uptake and $K_{i,j} < 1$ indicates discrimination against the trace component. The "soil" in Eq. (2) has been variously defined as the bulk soil composition, exchangeable cations or soil pore waters (Poszwa et al., 2000; Tyler, 2004; Page et al., 2008). Soil pore water is the most readily available source of plant nutrients (Wyttenbach et al., 1995) and used in this study to characterize plant/soil fractionation. The "plant" in Eq. (2) consists of roots, stems and leaves which fractionate nutrients as they move up the transpiration stream (Marschner, 1995). Plant compositions also change during the growth cycle as indicated by the "spiking" of K concentrations earlier in the growth season relative to Ca and Mg (Fig. 2).

Wide ranges in experimental $K_{Sr/Ca}$ values are reported for a variety of grass species and solute compositions ($K_{Sr/Ca} = 0.8$–1.5; Veresoglou et al., 1996). $K_{Sr/Ca}$ values describing the fractionation between average grass and pore waters at various depths in the SCT 2, 3 and 5 soils are plotted in Fig. 7a–c. Fractionation factors are less than unity in the shallowest soils indicating discriminating against Sr relative to Ca by plants (SCT 2 = 0.82; SCT 3 = 0.78 and SCT 5 = 0.94). $K_{Sr/Ca}$ values decrease downward into the argillic horizon, below which they become relative constant ($K_{Sr/Ca=}$0.25–0.33), reflecting inputs from

Table 2
Elemental ratios and similarity factors S_{ij} (Eq. (1)) describing pore water trends above and below the biotic/abiotic interface. Data based on linear regression fits shown in Fig. 5.

	Biotic trends			Abiotic trends			Similarity S_{ij}		
	Sr/Ca	Mg/Ca	Na/Ca	Sr/Ca	Mg/Ca	Na/Ca	$S_{Sr,Ca}$	$S_{Mg,Ca}$	$S_{Na,Ca}$
SCT 2	0.0029	0.33	0.60	0.0071	2.45	22.9	0.404	0.135	0.026
SCT 3	0.0031	0.41	0.89	0.0074	3.40	42.8	0.425	0.119	0.021
SCT 5	0.0019	0.36	1.56	0.0079	2.69	20.7	0.242	0.133	0.075

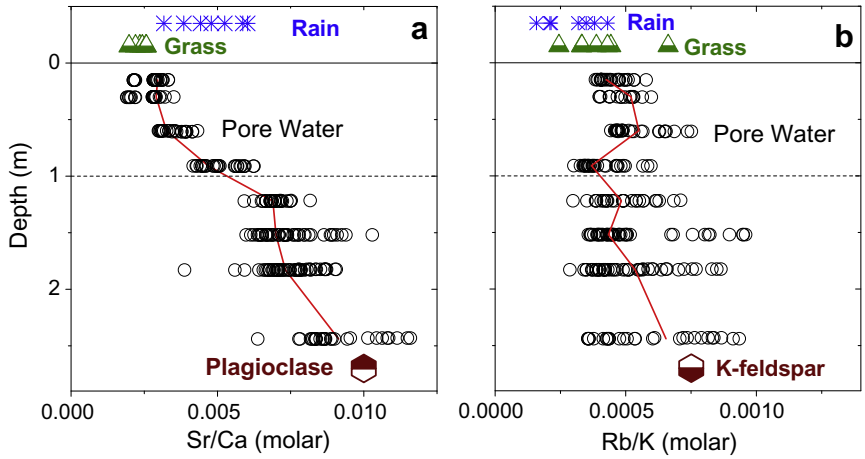

Fig. 6. (a) Sr/Ca and (b) Rb/K ratios in various components of the SCT 5 soil (partial listing of pore waters, grass and rain data in Appendices B and C; plagioclase and K-feldspar data from White et al. (2008a). Solid lines correspond to pore water averages at specific depths Dashed horizontal lines correspond to the approximate depth of maximum clay contents and the A/B interface (Fig. 3c–e).

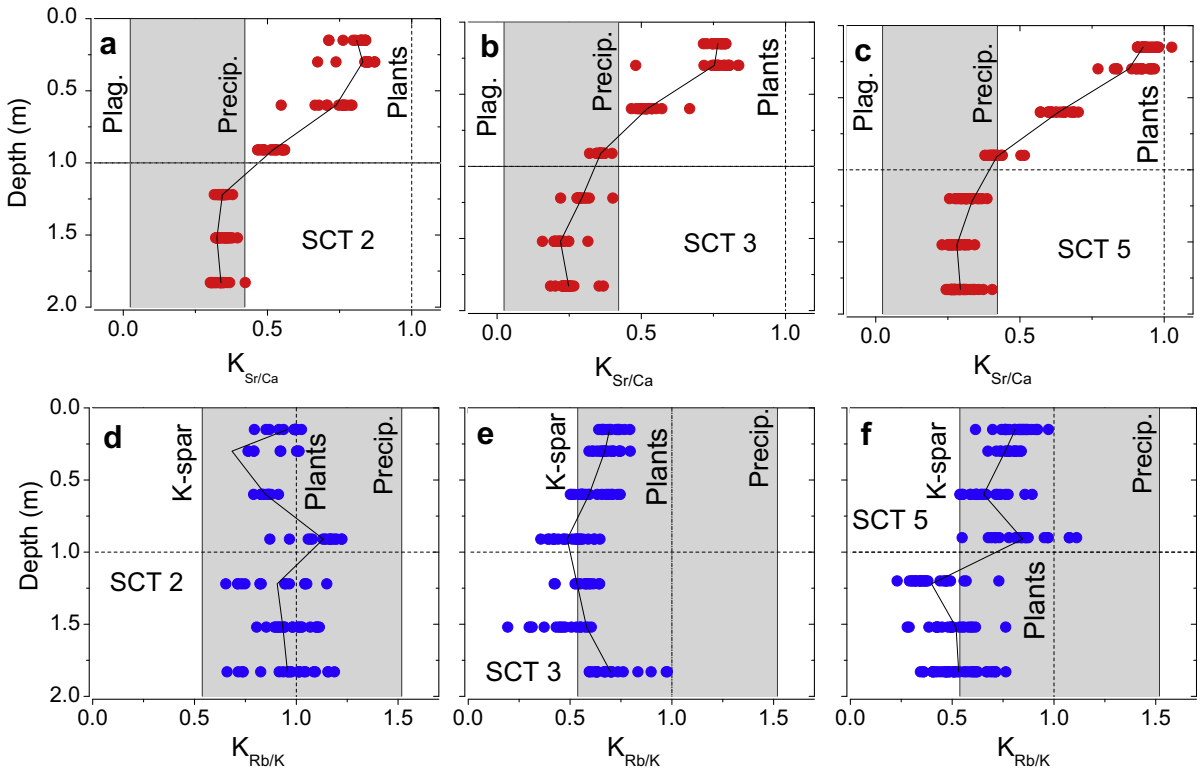

Fig. 7. $K_{Sr/Ca}$ and $K_{Rb/K}$ fractionation factors (Eq. (2)) describing the distributions of Sr/Ca (a–c) and Rb/K (d–f) between pore waters and plants in the SCT 2, SCT 3 and SCT 5 soils. Connected solid lines are average fractionations for pore waters at specific depths. Dashed vertical lines represent zero fractionation relative to plants. Shaded areas are range of possible fractionation factors produce by inputs from precipitation ($K_{Sr/Ca} = 0.42$ and $K_{Rb/K} = 1.52$) and mineral weathering ($K_{plag,\,Sr/Ca} = 0.0024$ and $K_{Kspar,\,Rb/K} = 0.54$). Dashed horizontal lines correspond to the approximate depth of maximum clay contents and the A/B interface (Fig. 3c–e).

precipitation and plagioclase weathering (shaded areas in Fig. 7a–c).

$K_{Rb/K}$ fractionation factors (Eq. (2)) are plotted in Fig. 7d–f. Average $K_{Rb/K}$ values between plants and the shallowest pore waters at 0.15 m are less than unity (SCT2 = 0.96, SCT 3 = 0.75 and SCT 5 = 0.82) in agreement with the literature consensus that Rb is excluded relative to K from biological materials (Kabata-Pendias and Pendias, 2001). $K_{Rb/K}$ values do not significantly increase with soil depth, generally falling in the range expected for a mixture of inputs from precipitation and K-feldspar weathering (shaded areas in Fig 7d–f).

4. DISCUSSION

Mineral nutrients in shallow pore waters more strongly reflect biotic processes while deeper pore waters reflect abiotic processes, principally chemical weathering (Richter and Markewitz, 1995). Soil studies commonly do not consider the transition zones where these processes are of similar importance and where major nutrient transfers occur. Such transfers may occur under open conditions in which plant nutrients reflect a balance between abiotic inputs from atmospheric and weathering and losses by pore water discharge. Alternately, transfers can occur under closed conditions where these external inputs and outputs are minimized and nutrients are repeatedly cycled between the biomass and shallow soils (Burnham, 1989).

4.1. Defining the biotic/abiotic (A/B) interface

Both solute distributions, and the abiotic and biotic processes that produce them, are defined in terms of soil gradients as shown in the schematic in Fig. 8. Abiotic processes, dominated by chemical weathering, produce positive soil gradients, i.e., solutes generally increase with depth due to increases in reactive mineral abundances, as well as downward hydrologic gradients which produce longer flow paths and reaction times (Brantley and White, 2009). These parallel gradients are also shown to increase linearly with soil depth (Fig. 8). Increases in pore water Na with depth in the SCT 2 and SCT 5 soils (Fig. 4) are specific examples of abiotic gradients dominated by plagioclase weathering. The characterization of solute, mineral and hydrologic gradients and their interpretation in terms of chemical weathering rates has been previously addressed for the Santa Cruz soils (White et al., 2008a, 2009; Maher et al., 2009).

Solutes dominated by biological processes are expected to vary seasonally, encompassing a range in gradients shown schematically by the shaded triangular area in Fig. 8. Gradients are positive, i.e., solute increase downward in the soil during active plant growth, reflecting nutrient extraction by a higher density of roots at shallower depths. Solute gradients become reversed, i.e., solutes concentrations increase upwards during annual dieback when root decay and leaching of above-ground litter reintroduces soluble nutrients back into the shallow soils. This redistribution is aided by bioturbation and microbial degradation, processes which decrease in intensity with soil depth (Perg et al., 2001; Moore et al., 2009). The large variations in shallow pore water K and Ca in the SCT 2 and SCT 5 soils are examples of biotic solute gradients dominated by seasonal growth patterns (Fig. 4).

The *biotic/abiotic (A/B) interface* is defined in this paper as the soil horizon where the abiotic/biotic gradients intersect (horizontal line in Fig. 8). With increasing depth below this interface, abiotic processes progressively dominate over biotic process in controlling solute distributions and above this interface, biotic processes progressively dominate over abiotic progresses.

The A/B interface correlates pedologically in the Santa Cruz soils with argillic horizons dominated by fine-grained, poorly-crystalline kaolinite (White et al., 2008a). These argillic horizons are readily identified in the field by mottled red/grey peds that reflect variable concentrations of associated Fe-oxyhydroides (Schulz et al., 2010). While these argillic horizons thicken with soil age, maximum clay contents remain constant at about one meter (Fig 3c–e), a depth used

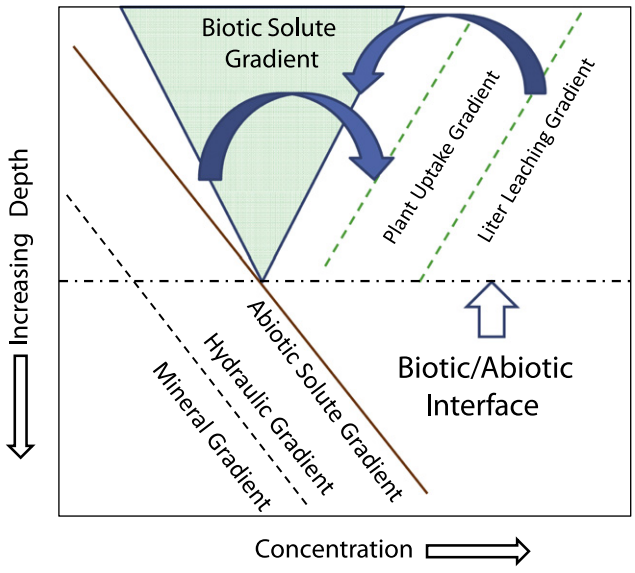

Fig. 8. Schematic illustrating relationships between biotic and abiotic soil gradients (soil depth on the vertical axes and solute concentrations or intensities on the horizontal axes. Positive hydraulic and residual mineral gradients control the abiotic solute gradient. Nutrient uptake by increasing root densities with shallower depths (right facing arrow) produces residual positive solute gradients during the growing season. Additions of nutrients to pore waters by leaching of plant litter during die back (left facing arrow) produce reversed negative biotic solute gradients. The seasonal variation in the biotic gradients is contained in the triangular area. The biotic/abiotic (A/B) interface is shown by the horizontal line.

in the following discussion to approximate the A/B interface. The A/B interface strongly influences both spatial and temporal distributions of solute mineral nutrients, (Figs. 5 and 9), correlates to the lower boundary for plant roots and impacts seasonal soil moisture variability (Fig. 3).

Elluvation, eolian deposition, bioturbation and fluctuations in ground water tables are cited causes for the formation of soil argillic horizons (Phillips, 2007). However, the inverse correlation between biological activity and clay formation with depth in the Santa Cruz soils is probably not casual but reflects a coupled relationship between biotic and abiotic processes (Maher et al., 2009; White et al., 2009). Pore waters, close to kaolinite thermodynamic saturation within the argillic horizon, are significantly supersaturated in the overlying shallow soils due to much higher solute Al concentrations (White et al., 2009). High Al commonly denotes organic complexation and colloid formation (Driscoll et al., 1985; Boudot et al., 1996). The loss of DOC by microbial activity in the Santa Cruz soils (Moore et al., 2009) results in declining organic Al complexation with depth, increasing concentrations of monomeric Al and the saturation and precipitation of kaolinite at the biotic/abiotic interface (Maher et al., 2009). These coupled interactions produce argillic horizons that become self-perpetuating features, the intensities of which increase with soil age in the chronosequence. Other studies relating the formation of clay to biological processes are summarized by Velde and Barré (2010).

4.2. Seasonal cation variations above and below the biotic/abiotic interface

Large seasonal variations in shallow solute cations occur above the A/B interface due to nutrient cycling while much smaller seasonal variations occur below the A/B interface (Figs. 4 and 8). These differences are further refined by considering only the fraction of a solute nutrient affected by biologic uptake and release $c_{j,bio}$

$$c_{j,bio} = c_{j,pw}\left[\frac{c_{Cl,precip}}{c_{Cl,pw}}\right] - c_{j,precip} \quad (3)$$

where $c_{Cl,precip}$ and $c_{j,precip}$ are average rainfall concentrations and $c_{Cl,pw,\ j,pw}$ are the measured concentrations in pore water (data in Appendix B). Pore water Cl is assumed to be derived solely from precipitation and excluded during nutrient uptake by the roots (Marcum, 2001). Eq. (3) corrects total pore water solutes for inputs from precipitation and the subsequent concentration by ET but not for chemical weathering whose inputs are expected to be relatively small and show only minor seasonal variability. Note that $c_{j,bio}$ (Eq. (3)) is positive or negative depending on specific cation behavior.

Seasonal variations in the biotic component ($c_{j,bio}$) of SCT 5 pore waters sampled over three yearly growth cycles from above and below the A/B interface (0.15 and 1.22 m) are shown in Fig. 9 (data in Appendix C). Less intense sampling at the other soil sites indicate similar pore water distributions. In the shallower soil, highest Ca, K and Mg

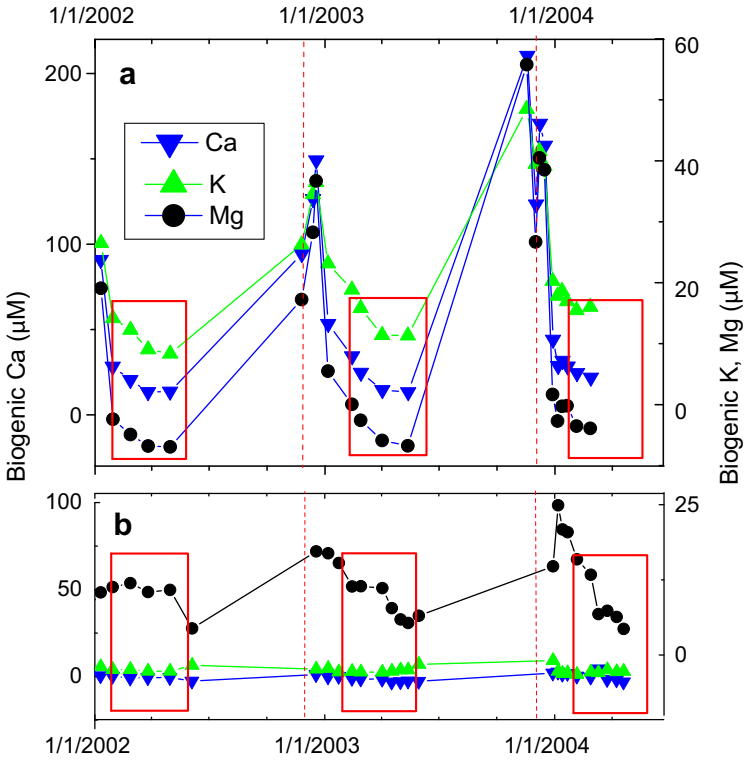

Fig. 9. Seasonal variations in the biotic component of pore water cations ($c_{j,bio}$ in Eq. (3)) sampled at depths of (a) 0.15 and (b) 1.20 m in the SCT 5 soil. Pore waters within rectangular boxes correspond to periods of maximum plant growth (January to April of each year). Vertical dashed lines correspond to first significant rain of each year.

($c_{j,bio}$) occur after the first rains in November and December (dashed vertical lines in Fig. 9a) and correspond to rapid leaching of decayed plant litter as shown experimentally by Fraysse et al. (2010). Solute Ca, K and Mg rapidly decline after the initiation plant growth and reach minimum levels at the end of growing season in May and early June of each year (the growing seasons are bracketed by the red rectangular boxes in Fig. 9). These solute declines are the exact opposite of Ca, K and Mg increases in the biomass measured during the same period (Fig. 2). During the following dry season, the dead biomass degrades, producing a labile nutrient fraction which again rapidly leaches into the pore water during the first fall rains of the next wet season.

On an annual basis, Ca is almost completely cycled, exhibiting high $c_{Ca,bio}$ at the beginning of the growing seasons and declining to near zero at the end of plant growth (Fig. 9a). Magnesium exhibits small negative $c_{Mg,bio}$ values by the end of the each growing season. Although Mg is not generally considered a limiting mineral nutrient, plants are extracting Mg in excess of what was previously contributed from leaching of plant litter. This net loss does not reflect the relatively large abiotic Mg inputs from marine aerosols dissolved in precipitation (Eq. (3)).

Declines in the biogenic K in shallow pore waters are proportionally less than for Ca and Mg, resulting in larger residual $c_{k,bio}$ at the end of the growing season (data within boxes in Fig. 9a). Incomplete K cycling appears at odds with its role as a limiting nutrient in many grassland ecosystems (Barger et al., 2002; Smit et al., 2002). Incomplete K cycling via the pore waters may reflect the fact that in some grasslands K is rapidly recycled via leaf litter and soil organics, in contrast to Mg and Ca which are cycled through root senescence, resulting in greater pore water interaction (Perez and Franci, 2007).

Biologically cycled K and Ca ($c_{j,bio}$ in Eq. (3)) are much lower and exhibit essentially no seasonal variabilities in pore waters below the A/B interface (1.2 m data in Fig. 9b). This correlates with the spatial separation of biotic and abiotic pore water trends (Fig. 5) and indicates that these major nutrients are strongly retained above the A/B interface. Magnesium ($c_{Mg,bio}$ in Eq. (3)) is proportionally much higher that Ca and K below the A/B interface, exhibiting the same variability as it does at 0.15 m, albeit with lesser seasonal extremes (Fig. 9b). This implies that Mg is not as strongly retained within the biotic soil horizons as are K and Ca. Leakage across the A/B interface is reflected in the more diverse trends in pore water Mg/Ca ratios, particularly for the older SCT 5 soil (Fig. 5) and accounts for the small net deficiencies of biotic Mg ($c_{Mg,bio}$) at the end of the growing season in the shallower soils (Fig. 9a). The lack of a strong retention of Mg, compared to Ca and K, is probably related to larger precipitation inputs (Appendix C) and lower plant nutrient requirements (Table 2).

4.3. Elemental fractionation and closed nutrient cycling

Elemental fractionation between the bulk vegetation and pore waters (Eq. (3)) is expected to be seasonally constant under open system conditions where the pore water reservoir is large and/or a dynamic balance is maintained between plant growth and external nutrient inputs and outputs. In contrast, fractionation between pore waters and bulk vegetation will vary seasonally under closed system conditions when there is a substantial feedback in total nutrients between the plants and the soils. Selective extraction during plant growth will change the proportions of mineral nutrients in pore waters which, in turn, will impact their proportions in the accumulating biomass.

Assuming closed conditions, pore waters Sr/Ca and Rb/K distributions are described by Rayleigh-type fractionation (Faure and Mensing, 2005), similar to that used in isotopic studies of plant nutrients (Ding et al., 2008)

$$\frac{[C_i/C_j]}{[C_i/C_j]_{inital}} = \left(C_j/C_{j,\ inital}\right)^{(K_{i,j}-1)} \quad (4)$$

While Eq. (4) assumes irreversible uptake via a reactant, i.e., plants, only changes in solute concentrations are considered, thus removing the issue of measuring bulk versus incremental biomass accumulation over the growing season.

Calcium and Sr concentrations (C_i and C_j) and corresponding [Sr/Ca] and [Rb/K] ratios measured in the shallowest pore water (0.15 m) at all five sites are normalized against initial compositions sampled the beginning of the growth cycles (Eq. (4)). While exhibiting significant variability, normalized Sr/Ca and Rb/K ratios increase with decreasing amounts Ca and K (Fig. 10), consistent with the increasing retention of solute Sr and Rb as plants progressively extract Ca and K ($K_{Sr/Ca}$ and $K_{Rb/K} < 1$ in Fig. 7).

Pore water data are compared to predicted Rayleigh fractionation trends (Eq. (4)) based on the fractionation factors shown in Fig. 10. Fractionation is bounded by flat lines ($K_{Sr/Ca}$ and $K_{K,Rb} = 1$) indicating no Sr and Rb discrimination by the plants, and by steep concave curves indicating the complete exclusion of Sr and Rb by the plants ($K_{Sr/Ca}$ and $K_{K,Rb} = 0$). Intermediate curves are generated using an value of 0.85 which approximates the average $K_{Sr/Ca}$ and $K_{K,Rb}$ values for Sr/Ca and Rb/K fractionation shown in Fig. 7.

Rayleigh fractionation describing closed uptake by plants is only one half of the annual nutrient cycle. Reverse changes in solute Sr/Ca and Rb/K ratios occur as nutrients are reintroduced back into the soils from litter leaching after plant dieback. Unlike nutrient uptake, reflecting continuous fractionation, back titration of litter involves constant Sr/Ca and Rb/K ratios reflecting elemental proportions incorporated into the bulk biomass relative to residual amounts remaining in the pore water at the end of the growing season.

For complete transfer, C_i/C_j in the final bulk biomass will equal $[C_i/C_j]_{inital}$ in the pore water (Eq. (4)), a situation approached for Ca at the end of successive growing seasons (Fig. 9a). On average, 95% of the Ca is removed from the pore water, resulting in a mixing line that is initially steep and then rapidly approaches pore water $[Sr/Ca_j]_{initial}$ (Fig. 10a). Conversely, about 80% of the K is extracted from the pore water by the end of successive growing

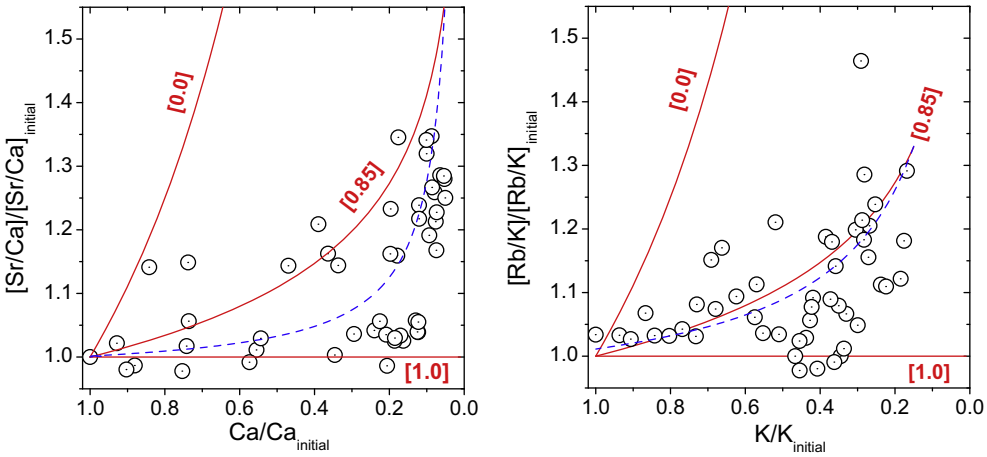

Fig. 10. Changes in pore water Sr/Ca and Rb/K ratios plotted against declines in residual Ca and K concentrations during plant growth. Data points correspond to measured values for pore waters in the shallowest soil sites (0.15 m; inclusive of all sites). Solid lines describe closed system Rayleigh fractionation during nutrient uptake by plants (Eq. (4)) based on indicated fractionation factors (Eq. (3)). Dashed lines describe mixing resulting from subsequent leaching of plant litter.

seasons (Fig. 9a), producing a mixing line with an initially shallower slope that more closely retrace the fractionation lines describing Rb/K uptake (Fig. 10b). While the predicted fractionation/mixing trends are obvious over-simplifications, these relationships approximate seasonal distributions of Sr/Ca and R/K ratios measured in shallow pore waters.

4.4. Nutrient balances

Nutrient balances, an important issue relating to the soil sustainability, are addressed using a simple flow chart (Trudgill, 1988). Mineral nutrient reservoirs in Fig. 11a are shown as boxes (mole m^{-2}). Irreversible fluxes are shown as single arrows and reversible fluxes as double arrows (mmoles m^{-2} yr^{-1}). All parameters in Fig. 11a are normalized to 1 m^2 of land surface, and for the soils, are integrated to a depth of 2.5 meters, encompassing the biotic and abiotic soil horizons that bracketed by the A/B interface. Numerical results (presented for the SCT 5 site in Fig. 11a and summarized for the other soils in Table 3) incorporate plant and pore water data presented in this paper, along with previously reported information on mineralogy, weathering rates, hydrology and cation exchange (White et al., 2008a,b, 2009; Maher et al., 2009).

Soil minerals are the largest cation reservoir in the soils (Fig. 11a). Potassium, the dominant cation, is contained in residual feldspars with lower amounts of Na and Ca present in plagioclase and Mg contained in detrital smectite (White et al., 2008a). The exchange substrate is the second largest reservoir (Fig. 11a), dominated by Ca and Mg sorption onto clays (White et al., 2009). The plant and pore water reservoirs are of comparable size but are orders of magnitude smaller than the mineral and exchange reservoirs.

The reversible biological fluxes to and from pore waters ($q_{j,bio}$) are based on annual above-ground AANPs (Table 1). Annual K fluxes are more than an order of magnitude greater than the solute K reservoir, thus precluding pore water as the primary nutrient source for plants. In contrast, biomass Ca and Mg fluxes are comparable, making pore water a viable but seasonally variable source for plant nutrients. Biogenic Na fluxes are low compared to the amount in pore water, indicating that only small proportions are annually extracted by the plants.

Precipitation inputs ($q_{j,precip}$) equal the product of average rainfall and corresponding solute concentrations (data in Appendix C and from White et al., 2009). Input fluxes from chemical weathering ($q_{j,weather}$) are calculated from elemental differences in the present-day soils and the initial protolith divided by the terrace age (weathering data and calculations from White et al., 2008a, 2009). Inputs fluxes are dominated by Na from plagioclase weathering (Fig. 11a and Table 3). Weathering fluxes for other elements are relatively small compared to the pore water and plant reservoirs.

Elemental losses resulting from pore water discharge $q_{j,discharge}$ (Fig. 11a) are products of the hydraulic flux q_h (m m^{-2}) and solute concentrations $C_{j,pw}$ at 2.5 m. The hydraulic flux equals the difference between $q_{precip.}$ and the evapotranspiration flux q_{ET} (White et al., 2009).

$$q_h = q_{precip.} - q_{ET} = q_{precip}\left(\frac{c_{Cl,precip.}}{c_{Cl,pw}}\right) \quad (5)$$

The ET flux, in turn, is proportional to the ratio of Cl in precipitation and pore water at 2.5 m (Eq. (3)). Precipitation ($q_{precip.} = 0.59$ m yr^{-1}) and ET ($q_{ET} = 0.46$ m yr^{-1}) fluxes result in a net downward hydraulic flux ($q_h = 0.13$ m yr^{-1}) through the SCT 5 soil column (Eq. (5) and Fig. 11a). Fluxes for the other soil sites are reported in Table 3. Corresponding solute discharge fluxes ($q_{j,discharge}$) are dominated by Na and Cl, reflecting large inputs from weathering and/or precipitation (Fig. 11a and Table 3). Solute discharges for K, Ca and Mg are significantly less than Na. Note that Cl fluxes in rainfall and discharge fluxes are equal based on Cl conservancy assumed in Eq. (5).

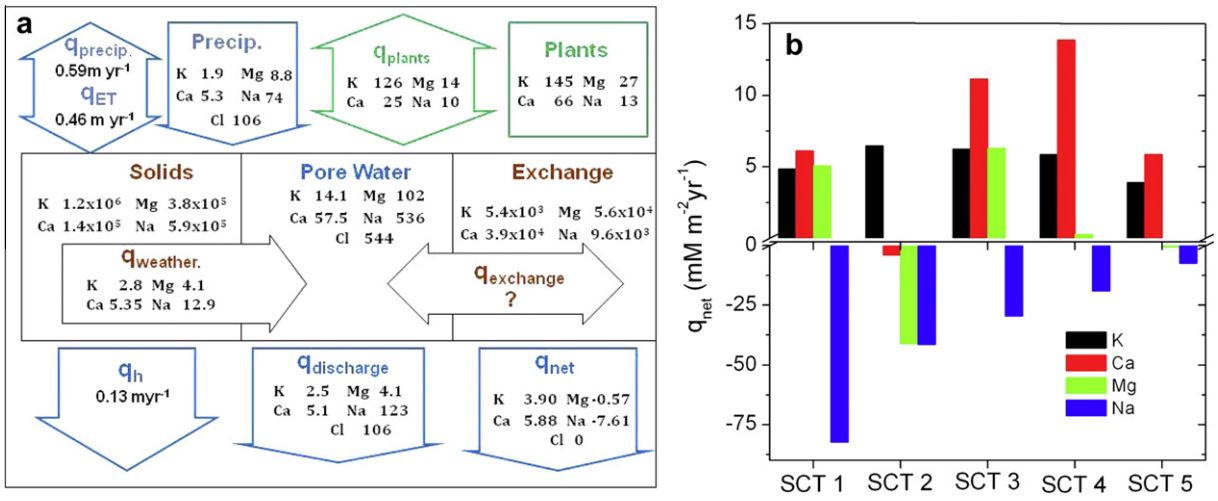

Fig. 11. Soil nutrient balances (a) Schematic showing elemental fluxes (mmoles m^{-2} yr^{-1}) between soil and plant reservoirs (mmoles m^{-2}) at the SCT 5 site. Soil values are integrated to a depth of 2.5 m. Biomasses and fluxes are from Table 1 and Appendix B. Mineral masses and weathering fluxes are based on data from White et al. (2008a) and exchangeable cations are from White et al. (2009). Note that the exchange flux $q_{j,exchange}$ (extent of exchange equilibrium) remains undefined. Water balances between rain (q_{precip}), evapotranspiration (q_{ET}) and discharge ($q_{discharge}$) are based on Eq. (5) and data from White et al. (2009). (b) Positive net nutrient fluxes for the five terrace soils (q_{net} in Eq. (8)) indicate net retention and negative values net losses from the soil.

Table 3
Major cation fluxes (moles m^{-2} yr^{-1}) described in Fig. 11a and by Eqs. (5) and (8) and fractions of nutrients cycled under closed conditions (F_{plant}, Eq. (6)).

	K	Ca	Mg	Na	K	Ca	Mg	Na	K	Ca	Mg	Na
$q_{j,plants}$					$q_{j,precip.}$				$q_{j,weather.}$			
SCT1	499	42.0	39.1	159	2.69	4.98	10.4	89.6	2.63	4.65	3.74	7.51
SCT2	207	40.6	30.3	21.9	3.98	5.39	12.9	113	3.81	13.3	15.1	18.4
SCT3	247	40.2	27.8	58.7	4.43	8.66	12.1	83.9	2.95	5.57	6.84	15.1
SCT4	297	78.5	42.0	54.5	4.28	10.1	13.7	85	3.56	7.63	4.50	14.9
SCT5	252	49.1	27.7	20.5	1.96	5.33	8.82	74.8	2.57	5.13	4.08	12.9
$q_{j,discharge}$					$q_{j,net}$				$F_{j,plants}$			
SCT1	0.47	3.50	9.06	179	4.85	6.13	5.08	−82.3	1.00	0.92	0.81	0.47
SCT2	1.30	22.6	69.0	172	6.49	−3.88	−41.0	−41.3	0.99	0.64	0.31	0.11
SCT3	1.12	3.06	12.6	129	6.25	11.2	6.30	−29.6	1.00	0.93	0.69	0.31
SCT4	1.96	3.90	17.9	119	5.88	13.9	0.27	−19.1	0.99	0.95	0.70	0.31
SCT5	0.63	4.57	13.5	95.2	3.90	5.88	−0.57	−7.48	1.00	0.91	0.67	0.18

4.5. Closed versus open nutrient outputs

The extent to which mineral nutrients behave under close conditions in the shallow soils is quantified by the parameter $F_{j,plants}$ which is the fraction of a nutrient flux $q_{j,plants}$ cycled by the vegetation compared to the sum of the fluxes, $q_{j,plants}$ and $q_{j,discharge}$.

$$F_{j,plants} = \frac{q_{j,plants}}{q_{j,plants} + q_{j,discharge}} \quad (6)$$

$F_{j,plants} = 1$ denotes complete retention and $F_{j,plants} = 0$ denotes complete loss from the soil. Average values of $F_{K,plants} = 0.99$ and $F_{Ca,plants} = 0.92$ (Table 3) indicate closed conditions as suggested by the retention of seasonally cycled K and Ca above the A/B interface (Fig. 9) Average $F_{Mg,plants} = 0.62$, indicates that comparable portions of Mg are recycled through the plants and lost to discharge below the A/B interface (Fig. 9). An average $F_{Na,plants} = 0.26$, indicates that only a small proportion of Na is retained by the plants and that the largest proportion is directly discharged through the soils.

Nutrient retention in the shallow soils, an obvious benefit to plants, involves micro-scale interactions between pore waters, roots and the rhizosphere (Cardon and Whitbeck, 2007). These processes must be very efficient, having to compete against downward pore water transport and nutrient losses to deeper soils beneath the rooting zone. Average downward pore water transport is significant; advective fluxes calculated by dividing q_h (Eq. (5)) by the soil density, produces average pore water residence times of only about 3 years in the upper 2.5 m of the Santa Cruz soils (White et al., 2008a).

Continuous vertical infiltration (plug flow) produces pore waters that progressively evolve with depth from those

reflecting shallow biogenic processes to mixtures reflecting additional inputs from deeper mineral weathering. The spatial segregation of solutes into distinct trends above and below the A/B interface (Fig. 5) is best explained by the independent evolution from common dilute rainwater sources. Rapid drawdown of transient perched ground waters shortly after large winter storms indicates active recharge of dilute pore water through the argillic horizon (White et al., 2009). As the storm frequencies decrease and plant transpiration increases later in the spring, unsaturated soil conditions strongly retard further pore water infiltration (Stonestrom et al., 1998). Pore waters are rendered relatively immobile, being retained within separate soil horizons during much of the year, particularly during the period of maximum plant growth. These conditions promote closed system conditions in which solutes become free to evolve along separate biotic and abiotic pathways (Fig. 5).

4.6. Closed versus open nutrient inputs

The discussion assumes that precipitation and chemical weathering are the primary mineral nutrient sources for the vegetation (Fig. 11a). This assumption is now tested based on Rb/K and Sr/Ca ratios (Figs. 6 and 7) along with reported isotopic data describing $^{87}Sr/^{86}Sr$, $^{24}Mg/^{22}Mg$ and $^{44}Ca/^{40}Ca$ distributions in the Santa Cruz soils (Bullen et al., 2004; White et al., 2009; Tipper et al., 2010).

Plant/shallow pore water fractionation (Eq. (2)), reflecting biological discrimination against Rb, is shifted to the left of vertical dashed lines in Fig. 7d–e denoting zero plant fractionation ($K_{Rb/K} = 1$). These measured $K_{Rb/K}$ values plot intermediate relative to higher $K_{Rb/K}$ inputs reflecting hypothetical plant/precipitation fractionation and lower inputs reflecting plant/K-feldspar fractionation (vertical solid lines in Fig. 7d–e). Fractionation envelopes (shaded areas in Fig. 7d–e) correspond to ranges in plant-porewater $K_{Rb/K}$ values that reflect variable inputs from rain and weathering and modified by biological fractionation. While the proportions of these inputs appear relatively constant with increasing depth in the SCT 2 soil, plant-pore water $K_{Rb/K}$, values for the SCT3 and SCT 5 soils shift toward the left edge of fractionation envelope, indicating increased inputs from K-feldspar weathering at and below the A/B interface (dashed horizontal lines in Fig 7d and e).

Shallow plant/pore water $K_{Sr/Ca}$ values also plot to the left of the vertical plant line ($K_{Rb/K} = 1$ in Fig. 7d–e), indicating discrimination by plants against pore water Sr. However, $K_{Sr/Ca}$ values plot far to the right of the fractionation envelope defining inputs from precipitation and plagioclase weathering indicating that they are not acting as direct nutrient sources to the plants. Only below the A/B interface, do plant/pore water $K_{Sr/Ca}$ values plot within the input fractionation envelopes, reflecting the increased plagioclase weathering.

Nutrient inputs are further investigated by using fractionation factors based on reported isotopic data for Santa Cruz. $^{87}Sr/^{86}Sr$ ratios, reported in White et al. (2009), are normalized against internal standardizations such that any biologic fractionation potentially caused by small mass differences are removed from the analyses (Bullen and Eisenhauer, 2009). Plant-pore water $^{87}Sr/^{86}Sr$ ratios in the SCT 2 soil fall along a simple mixing line between inputs from radiogenically heavy rainfall, similar to seawater, and radiogenically light Sr reflecting plagioclase weathering (Fig. 12a).

$^{26}Mg/^{24}Mg$ data for the SCT 2 site (Fig. 12a, after Tipper et al., 2010) are reported as $\delta^{26}Mg$ relative to the DSM2 standard (Galy et al., 2003). $\delta^{26}Mg$ in rain exhibits consistent values (average $= -0.79$) which, like $^{87}Sr/^{86}Sr$, are equivalent seawater (Fig. 12b). $\delta^{26}Mg$ values for the shallowest pore waters (0.15 m) exhibited no discernable seasonal variation (average values $= -0.85$) and are only slightly lighter than rain. Pore water $\delta^{26}Mg$ increases with depth, reflecting inputs of isotopically heavy smectite ($\delta^{26}Mg = +0.11$; Tipper et al., 2010). Grass $\delta^{26}Mg$ data for the SCT 2 site averages +0.21 per mil heavier than rain and +0.27 per mil heavier than the shallowest pore waters (Fig. 12b).

$K_{^{24}Mg/^{22}Mg}$ values calculated from Eq. (3), after first converting $\delta^{26}Mg$ values into isotopic ratios based on the DSM2 standard, are shifted to the right of plant line ($K_{^{24}Mg/^{22}Mg} = 1$ in Fig. 12d), indicating preferential ^{24}Mg uptake by the plants. $K_{^{24}Mg/^{22}Mg}$ values (except for a single sample at 0.30 m) plot close to input fractionation for precipitation. With increasing depth, $K_{^{24}Mg/^{22}Mg}$ values cross into the fractionation envelope in response to the weathering of ^{24}Mg-depleted smectite. In spite of significant biologic fractionation, the trend in this data exhibits no deflection across the A/B interface (1 m) which is consistent with leakage of biogenic Mg into the deeper soil (Fig. 9b).

$^{44}Ca/^{40}Ca$ ratios for the SCT 1 soil (Bullen et al., 2004), normalized to sea water (Schmidt et al., 2003), are plotted as $\delta^{44}Ca$ values in Fig 12c. Average $\delta^{44}Ca$ in rain (-1.25) is significantly lighter than seawater, with individual samples exhibiting much greater variable than either $^{87}Sr/^{86}Sr$ or $^{26}Mg/^{24}Mg$ (Fig. 12a and b). Shallow pore water ($\delta^{44}Ca = -1.84$) is much lighter than precipitation but only slightly heavier than average grass ($\delta^{44}Ca = -2.02$).

Shallowest plant/pore water $^{44}Ca/^{40}Ca$ fractionation (Eq. (3)) is shifted slightly to the left of the plant line ($K_{^{44}Ca/^{40}Ca} = 1$ in Fig 12e) indicating biologic discrimination against heavier Ca as opposed to lighter Mg (Fig. 12d). However, plant/shallow pore water ($K_{^{44}Ca/^{40}Ca}$ values fall to the far right of the input fractionation envelope indicating that plant $^{44}Ca/^{40}Ca$ does not directly reflect weathering and/or precipitation inputs. While the exact right edge of this envelope is ill-defined due to the large variability of $\delta^{44}Ca$ of rain (-1.25 ± 0.45), plant $\delta^{44}Ca$ values are lower in all cases (Fig. 12c). Plant/pore water ($K_{^{44}Ca/^{40}Ca}$ values decrease with increasing depth, and as opposed to ($K_{^{24}Mg/^{22}Mg}$, exhibits a strong inflection at A/B interface. This reflects the fact that very little biogenic Ca is transported into the deeper soil (Fig. 8) where Ca becomes dominated by plagioclase weathering (Fig. 12e).

Plant/shallow pore water $K_{Rb/K}$ and ($K_{^{44}Ca/^{40}Ca}$ fractionation factors indicate that while K and to a lesser extent Mg, are strongly cycled by the plants (Fig. 9), these nutrients reflect open inputs from precipitation and weathering. Plant K is a mixture of both sources while plant Mg is

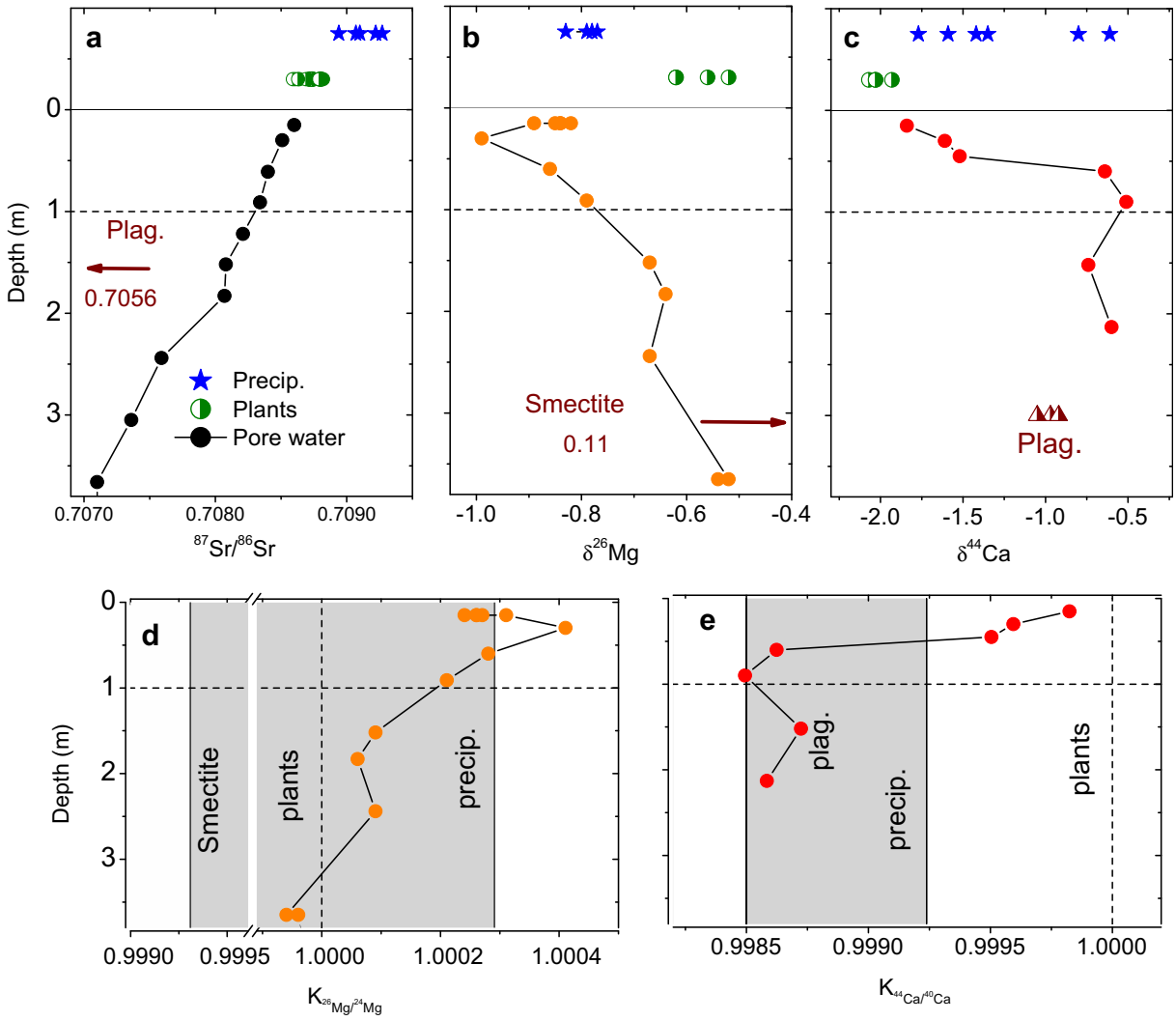

Fig. 12. Grasses, pore water and precipitation distributions for (a) $^{87}Sr/^{86}Sr$ data for the SCT 2 soil (White et al., 2009); (b) $^{26}Mg/^{24}Mg$ data for the SCT 2 soil (Tipper et al., 2010) and (c) $^{44}Ca/^{40}Ca$ data are for the SCT 1 (Bullen et al., 2004). Fractionation factors in (d) $K_{^{44}Ca/^{40}Ca}$ and (e) $K_{^{44}Ca/^{40}Ca}$ are based on Eq. (3). Dashed vertical lines represent zero fractionation relative to plants. Shaded areas are ranges of possible plant/pore water fractionation from mixtures of precipitation ($K_{^{44}Ca/^{40}Ca} = 0.99924$ and $K_{^{22}Mg/^{20}Mg} = 1.00029$) and mineral weathering (plagioclase $K_{^{44}Ca/^{40}Ca} = 0.99876$ and smectite $= K_{^{22}Mg/^{20}Mg} = 0.99931$). Horizontal lines correspond to approximate depth of maximum clay content and the A/B interface (see Fig. 3c–d).

dominated mostly by precipitation. These relationships are consistent with the relative sizes of K and Mg input fluxes from rainfall and chemical weathering (Fig. 11a and Table 3). In contrast, both plant/shallow pore water $K_{Sr/Ca}$ and ($K_{^{44}Ca/^{40}Ca}$ fractionation factors are significantly in excess of inputs from precipitation and weathering, implying that plants are not directly utilizing these Ca sources.

A lack of an apparent input source for plant Ca may be related a failure to fully characterize precipitation inputs. In an ongoing study, White et al. (2008b) found that Ca concentrations in rainfall correlate with specific storm tracks reflecting variable continental dust inputs from along the California coast. Such variability is reflected in the wide range in $\delta^{44}Ca$ values in precipitation (Fig. 12c). Aerosols in dry fall and fog during the summer months, which were not sampled for the present study, could potentially provide an unaccounted input source of isotopically heavy Ca.

An alternative explanation is that biologically cycled Ca, which is generally closed to downward leakage in pore water (Fig. 9), is also closed to significant inputs from weathering and precipitation. The same micro-scale processes enabling plants to tightly retain a specific nutrient may also isolate it from outside sources such as weathering and/or precipitation. While a prevention strategy against nutrient loss is beneficial to plants, the isolation from nutrient inputs is not.

The annual inputs of Ca from precipitation and weathering are about five times less than the amount of Ca contained in the plants (Fig. 11a and Table 3). If the cycling is completely open to Ca inputs, any differences currently observed in Sr/Ca and $^{44}Ca/^{40}Ca$ plant/pore water ratios would be lost in about five years. Alternately, if biologic cycling is effectively closed to both inputs and discharge, these differences would be maintained indefinitely. In fact, over

many grass growth cycles, fractionation could gradually shift away the external inputs to values approaching that of grasses, i.e., $K_{Sr/Ca}$ and ($K_{^{44}Ca/^{40}Ca} \rightarrow 1$ in Figs. 7d–f and 12e).

4.7. Nutrient balances

Regardless of extent to which an element behaves under open or closed conditions, the fluxes shown in Fig. 11a and listed in Table 3 should ideally balance (Velbel, 1995)

$$q_{j,precip} + q_{j,weather} \pm q_{j,exchange} \pm q_{j,plants} - q_{j,discharge} = 0 \quad (7)$$

Alternately, under non-ideal conditions, the extent of the imbalance $q_{j,net}$ is

$$q_{j,net} = q_{j,precip.} + q_{j,weather.} - q_{j,discharge} \quad (8)$$

assuming that the biological flux is conservative and the soil substrate is in exchange equilibrium ($q_{j,plants}$ and $q_{j,exchange} = 0$). Positive $q_{j,net}$ values indicate net nutrient retention and negative values net losses from the soils.

Net cation fluxes $q_{j,net}$ for all five terraces are listed in Table 3 and plotted as histograms in Fig. 11b. The largest imbalances occurs for Na, ($q_{Na,net} = -7$ to -82 mmoles m^{-2} yr^{-1}), undoubtedly reflecting the failure to account for total Na inputs from marine aerosols, as suggested by progressively larger negative $q_{Na,net}$ with decreasing distance from the coast (Figs. 1 and 11b). An ongoing study of precipitation patterns near Santa Cruz indicates that aerosols in dry fall and fog during the summer months may contribute upwards of a quarter of total NaCl to the soil waters (White et al., 2008b). The importance of such aerosol inputs are documented in other coastal environments (Whipkey et al., 2000).

Similar positive $q_{K,net}$ values for all five soils (3.9–6.5 mmoles m^{-2} yr^{-1}) indicate that K is being accumulated relative to inputs and discharge fluxes (Fig. 11b and Table 3). These net K increases are much smaller than the annual plant fluxes ($q_{K,plants}$ = 247–499 mmoles m^{-2} yr^{-1}). Ca is concentrated at comparable or higher levels than K in all but the SCT 2 soil ($q_{Ca,net}$ = 5.8–11.2 mmoles m^{-2} yr^{-1}). Net Mg retention, comparable to K and Ca in the younger soils, decreases to near zero in the older soils ($q_{Mg,net} = 5.1$ to -0.6 mmoles m^{-2} yr^{-1}). Both Ca and Mg exhibit anomalous losses from the SCT 2 soil (Fig. 11b; $q_{Ca,net} = -3.8$ and $q_{Mg,net} = -41.0$ mmoles m^{-2} yr^{-1} which correlate with significantly higher pore water Ca and Mg concentrations (compare SCT 2 and SCT 5 data in Fig. 4). The resulting large Ca and Mg discharge fluxes $q_{j,discharge}$ are only partly balanced by higher weathering rates (Table 3).

4.8. Longer-term environmental disequilibrium

The generally small positive K, Ca and Mg nutrient imbalances $q_{j,net}$ (excluding the SCT 2 soil), represent only 1–10% of the biologic fluxes $q_{j,plants}$ (Table 3). Thus, on an annual basis, these net fluxes do not substantially effect overall nutrient cycling. In the SCT 5 soil (Fig. 11a), an average of 10 years of net Ca accumulation and 50 years of net K accumulation are required to equal the amounts contained in the plant biomass. However, over longer times, net mineral nutrient accumulation is not sustainable; suggesting that present day soils may reflect longer-term environmental disequilibrium.

Any nutrient imbalance due to decadal scale effects, e.g., droughts or wildfires, or longer-term effects, e.g., climate change and vegetation succession must be interpreted in terms of the extent of exchange equilibrium with the mineral substrates. Note that the exchange term remains undefined in Fig. 11a. The mass of sorbed mineral nutrients are 2 to 3 orders of magnitude larger than any nutrient flux in the plant/soil system, thus providing a potentially large sink onto which mineral nutrients are being retained in the soil. For example, more than a thousand years of net K accumulation ($q_{K,net}$) and 5000 years of net Ca accumulation ($q_{Ca,net}$) are required to produce the amounts of these nutrients sorbed onto the mineral substrates. Such long-term exchange disequilibrium is contained in predictive models for acid rain recovery, suggesting that time scales of decades to centuries are required to reestablish base cation saturation (Driscoll et al., 2005). Even longer term disequilibrium, on time scales of hundreds of thousands of years, is suggested by $^{87}Sr/^{86}Sr$ data for other chronosequences (Bullen et al., 1997).

The long-term effect of plant successions on the Santa Cruz terraces is one environmental variable potentially impacting present day mineral nutrient imbalances. Holocene pollen records obtained near Santa Cruz document multiple transitions between oak-land and/or conifer forests and grassland ecosystems (Adam et al., 1981). The rooting depths of oaks and conifers are more than order of a magnitude deeper than the present day grasses (Stone and Kalisz, 1991), a difference that may have had profound effects on the depth of biotic/abiotic interface and present day exchange disequilibrium These variables may have had accelerated by human impacts, first by burning by Native Americans and latter by clearing and the introduction of exotic annual grasses by Europeans (Stromberg et al., 2007). More detailed studies on the relationships between long-term environmental disequilibrium, cation exchange capacities and soil mineral nutrient fluxes are clearly warranted.

5. CONCLUSIONS

This study investigates mineral nutrient interactions between temperate coastal prairie grasslands and soils in a chronosequence formed on uplifted marine terraces along coastal Central California. The relative simplicity of site, readily accessible small-scale vegetation, strong seasonal climate variability, definitive soil mineralogy and a span of soil ages, all provide an ideal opportunity to pursue an integrated study of the dynamics of the important mineral nutrients. A Mediterranean climate strongly regulates the annual growth pattern of dominantly exotic annual grasses. Above-ground biomass increases from late winter through spring, followed by subsequent die-back in the summer and fall. Annual net above-ground plant productivity (ANPP) is higher for the younger soils in the chronosequence compared to the older soils but generally bracket ANPP values cited for other temperate grasslands.

The biotic/abiotic (A/B) interface, an essential feature in explaining mineral nutrient dynamics, is defined as the intersection of chemical weathering gradients in the deeper soils and seasonal gradients reflecting biological cycling in the shallower soils. The A/B interface corresponds to argillic horizons, which contain maximum clay contents at soil depths of about one meter. The A/B interface is the lower boundary of plant roots and active mineral nutrient cycling in addition to the lower limit to significant bioturbation, carbon sequestration and microbial activity. It also serves as a physical and hydrologic barrier, confining significant moisture variability and evapotranspiration to the shallower soils.

Cation ratios in pore waters above the A/B interface fall along linear trends reflecting seasonal variability and preferential cycling of Ca relative Na, Mg and Sr. Solute ratios below the A/B interface fall along linear trends reflecting preferential release of Na, Mg and Sr relative to Ca produced by chemical weathering. The differences in these biotic/abioic trends decrease with elements of increasing chemical similarities (Sr/Ca > Mg/Ca > Na/Ca). Potassium does not reflect the same linear correlations as other cations due to thermodynamic saturation with respect K-feldspar and different pathways of uptake and/or leaching in the plants.

Shallow pore water K, Ca and Mg exhibit strong seasonal trends, high concentrations in the late fall and early winter, produced by leaching by plant litter by early rains, and low concentrations in the late spring corresponding to maximum uptake by the plants. Solute Ca declines to near-zero concentrations by the end of the growing season. Declines in K are proportionally less, reflecting different nutrient pathways, possibly directly through leaf litter decomposition and soil organics rather than through soil solutes. Shallow biogenic Mg exhibits negative values at the end of the growing season. Below the A/B interface, biologically-derived solute K and Ca remain low throughout the year and exhibit no seasonal variability. This contrasts to Mg which is proportionally higher and exhibit dampened seasonal variations. Leakage of Mg across the A/B interface results from higher marine aerosol inputs and lower nutrient requirement by the plants.

Plants discriminate against Sr and Rb, relative to Ca and K during growth, producing plant pore water fractionation factors $K_{Sr/Ca}$ and $K_{Rb/K}$ that are less than unity. The closed cycling of these nutrients is addressed based on a Rayleigh fractionation-mixing relationship. The source of mineral nutrients in plants is investigated by comparing these plant/pore water fractionation factors with predicted inputs from precipitation and chemical weathering. Results based plant/pore $K_{Rb/K}$ and $K_{^{24}Mg/^{22}Mg}$ (isotope data from the literature) indicate that, although K and to a lesser extent Mg are tightly cycled between plants and shallow pore waters, these nutrients ultimately reflect precipitation and weathering inputs. In contrast, plant/pore $K_{Sr/Ca}$ and $K_{^{44}Ca/^{40}Ca}$ values cannot be generated by these inputs, implying that not all input sources are accounted for, in particular marine aerosols in fog and dry fall. Alternatively the same processes that isolate nutrients from leaching by pore waters

Appendix A
Vegetation and associated characterisitcs at the SCT 2 and SCT 3 sites.

Soil site	Scientific name	Common name	Nitrogen fixing	Growth cycle[g]	Introduced or native	Growth habit	Max. rooting depths (cm)
3	*Briza major*	Large quaking grass	No	A	I	Grass	nd
2, 3	*Bromus diandrus*	Ripgut brome	No	A	I	Grass	80[a,b]
2	*Bromus hordeaceus*	Soft brome	No	A	I	Grass	80[a,b]
2, 3	*Lolium multiflorum*	Ryegrass	No	A, B, P	I	Grass	35[c]
2, 3	*Vulpia bromioides*	Brome fescue	No	A	I	Grass	40[d]
2	*Vulpia myuros*	Rat-tail fescue	No	A	I	Grass	40[d]
2	*Avena fatua*	Wild oat	No	A	I	Grass	91–160[e]
2, 3	*Linum bienne*	Pale flax	No	A, B, P	I	Forb	30–35[e]
2	*Plantago lanceolata*	Narrowleaf plantain	No	A, B, P	I	Forb	nd
2	*Raphanus sativus*	Radish	No	A	I	Forb	nd
2	*Rumex acetosella*	Sheep sorrel	No	P	I	Forb	150[f]
2	*Rumex pulcher*	Fiddle dock	No	P	I	Forb	nd
3	*Sidalcea malvaeflora*	Checker bloom	No	P	N	Forb	nd
2, 3	*Trifolium subterraneum*	Clover	Rhizobium	A	I	Forb	nd
2, 3	*Vicia sativa*	Garden vetch	Yes	A	I	Forb	nd

[a] Thill et al. (1984).
[b] Shaffer et al. (1994).
[c] Murphy et al. (1994).
[d] Beyrouty et al. (1990).
[e] Handi et al. (1988).
[f] Duke (1997).
[g] A = annual; B = biennial; P = perernial.

Appendix B
Above-ground biomass and elemental compositions of bulk vegetation.

Date	Mass (g m^{-2})	K (%)	Ca (%)	Mg (%)	Na (%)	P (%)	Si (%)	C (%)	S (%)	N (%)	Mn (ppm)	Cu (ppm)	B (ppm)	Zn (ppm)	Fe (ppm)
SCT 1 (Site)															
10/29/02	417	0.59	0.77	0.204	0.418	0.190	0.78	38.6	0.236	0.76	0.55	4.1	23.0	36.6	905
11/25/02	208	0.13	0.53	0.098	0.065	0.066	0.75	42.4	0.061	0.52	0.30	6.5	15.3	14.5	589
01/29/03	398	1.59	0.45	0.138	0.247	0.246	0.96	43.4	0.111	0.95	0.54	8.9	12.2	18.1	523
03/06/03	353	1.99	0.44	0.120	0.251	0.272	1.08	42.6	0.144	1.68	0.35	5.2	8.5	16.9	127
04/09/03	556	1.64	0.33	0.099	0.245	0.221	1.08	42.5	0.135	1.23	0.50	4.9	9.2	16.0	119
05/01/03	673	1.69	0.27	0.094	0.337	0.191	0.95	42.1	0.120	0.93	0.64	4.6	5.3	11.0	45
05/13/03	791	1.27	0.25	0.086	0.248	0.169	nd	43.1	0.089	0.90	0.62	9.1	5.7	11.8	58
06/10/03	684	1.02	0.32	0.111	0.367	0.173	0.78	42.8	0.139	0.80	0.53	7.0	6.6	14.0	249
07/29/03	724	1.17	0.28	0.084	0.464	0.132	1.39	41.9	0.094	0.47	0.61	3.8	5.7	9.7	54
08/27/03	546	1.11	0.33	0.107	0.383	0.141	1.32	41.8	0.103	0.52	0.51	7.5	6.8	13.8	89
09/23/03	422	1.18	0.41	0.119	0.578	0.145	0.88	42.6	0.116	0.51	0.53	4.4	10.5	16.4	133
11/11/03	479	0.20	0.34	0.079	0.476	0.107	1.39	44.0	0.064	0.43	0.35	3.2	5.6	18.6	228
SCT 2 (Site)															
10/20/02	312	0.13	0.57	0.087	0.030	0.034	0.68	44.3	0.060	0.44	0.72	5.2	9.3	16.1	274
11/13/02	599	0.13	0.75	0.098	0.025	0.050	0.73	43.5	0.070	0.73	1.54	6.0	10.6	21.5	479
12/11/02	401	0.75	0.72	0.127	0.060	0.087	0.95	43.7	0.092	1.01	1.28	7.3	11.5	25.3	583
01/06/03	225	1.03	0.51	0.124	0.106	0.084	0.74	43.4	0.096	1.06	0.52	6.2	10.4	19.9	271
03/06/03	495	0.96	0.52	0.118	0.066	0.114	0.79	43.9	0.116	1.21	1.60	6.7	7.3	19.3	220
04/02/03	714	0.74	0.43	0.096	0.066	0.091	1.17	43.5	0.110	1.07	1.97	6.0	5.8	17.6	185
05/01/03	1002	0.70	0.37	0.088	0.049	0.077	0.69	43.8	0.091	0.76	2.69	6.9	5.6	15.0	177
05/13/03	782	1.00	0.37	0.088	0.081	0.074	0.69	43.2	0.088	0.86	1.96	6.3	8.0	15.9	91
05/30/03	655	0.65	0.35	0.076	0.064	0.054	0.82	43.9	0.085	0.65	1.31	5.5	6.4	13.2	244
06/10/03	737	0.48	0.43	0.086	0.055	0.053	1.02	44.1	0.084	0.54	2.22	5.5	5.3	15.3	178
07/01/03	633	0.67	0.45	0.103	0.093	0.051	0.97	44.3	0.074	0.53	2.02	5.1	7.1	15.6	110
07/29/03	500	0.56	0.40	0.081	0.084	0.036	0.91	43.0	0.086	0.52	1.25	5.0	5.5	13.9	242
08/27/03	635	0.85	0.40	0.105	0.090	0.059	0.82	44.2	0.082	0.53	2.05	7.2	6.2	16.5	78
09/23/03	471	0.73	0.26	0.080	0.175	0.018	0.80	43.9	0.083	0.64	0.55	5.6	5.9	14.6	304
10/01/03	391	0.53	0.46	0.089	0.082	0.050	0.55	44.3	0.080	0.32	0.77	5.6	7.6	17.3	245
SCT 3 (Site)															
10/20/02	141	0.16	0.41	0.088	0.031	0.037	0.61	45.5	0.058	0.47	0.17	4.9	10.9	16.0	251
12/11/02	211	0.36	0.45	0.104	0.034	0.046	0.54	45.0	0.070	0.63	0.33	5.4	9.3	19.6	580
01/03/03	231	0.92	0.38	0.116	0.090	0.079	0.58	44.1	0.108	1.08	0.40	7.4	16.4	22.6	493
01/24/03	254	0.93	0.41	0.117	0.071	0.079	0.85	43.1	0.107	1.01	0.55	7.7	13.3	23.2	877
03/21/03	417	0.98	0.40	0.106	0.079	0.076	0.61	43.3	0.131	1.37	0.63	6.8	10.3	19.9	530
04/09/03	395	0.99	0.39	0.105	0.090	0.074	0.66	44.0	0.118	0.91	0.63	5.4	8.2	17.3	190
04/22/03	420	1.27	0.35	0.117	0.098	0.088	0.53	43.7	0.128	1.14	0.70	6.4	8.3	20.6	302
05/07/03	561	1.00	0.31	0.099	0.133	0.065	0.62	43.9	0.101	0.72	0.78	5.4	6.3	19.0	258
05/20/03	441	1.06	0.54	0.126	0.059	0.106	nd	44.3	0.107	0.99	nd	7.1	12.4	20.3	112
06/05/03	530	0.93	0.40	0.126	0.103	0.059	0.54	44.3	0.109	0.73	1.05	5.2	9.7	16.6	99
06/27/03	383	0.72	0.27	0.086	0.133	0.041	0.75	41.4	0.084	0.53	0.53	5.2	12.9	17.2	163
07/26/03	464	0.84	0.39	0.110	0.173	0.032	0.61	43.7	0.102	0.55	0.78	5.1	9.9	17.4	288

(*continued on next page*)

Appendix B (*continued*)

Date	Mass ($g\ m^{-2}$)	K (%)	Ca (%)	Mg (%)	Na (%)	P (%)	Si (%)	C (%)	S (%)	N (%)	Mn (ppm)	Cu (ppm)	B (ppm)	Zn (ppm)	Fe (ppm)
08/12/03	418	0.68	0.35	0.094	0.170	0.027	0.56	44.6	0.087	0.45	0.58	4.1	6.0	14.0	168
SCT 4 (Site)															
10/20/02	138	0.19	0.29	0.140	0.043	0.023	0.52	45.3	0.06	0.37	0.54	3.4	10.5	17.5	229
01/03/03	316	0.38	0.32	0.102	0.068	0.040	0.56	44.0	0.07	0.66	0.64	4.4	11.4	18.9	861
01/24/03	251	0.42	0.25	0.097	0.051	0.038	0.55	43.3	0.08	0.60	0.46	4.2	6.8	16.3	852
03/21/03	272	1.50	0.35	0.128	0.168	0.079	0.57	43.9	0.13	0.91	0.67	5.1	11.8	21.2	647
04/09/03	236	2.32	0.39	0.155	0.232	0.109	0.49	44.3	0.14	1.04	0.77	5.2	10.3	23.3	166
04/22/03	420	1.67	0.41	0.130	0.126	0.103	0.41	43.6	0.11	0.99	0.65	5.1	8.7	19.2	259
05/07/03	463	1.33	0.62	0.155	0.083	0.105	0.53	43.6	0.11	0.91	1.31	6.1	14.2	24.1	449
06/05/03	530	1.29	0.41	0.142	0.142	0.050	0.49	44.6	0.10	0.62	1.35	4.4	9.2	21.3	205
08/12/03	389	0.32	0.26	0.115	0.045	0.039	0.52	44.2	0.07	0.60	0.82	3.5	9.4	16.7	664
10/01/03	340	0.87	0.27	0.118	0.132	0.027	0.58	44.7	0.08	0.40	0.61	3.3	8.7	18.4	217
10/30/03	367	0.70	0.27	0.122	0.130	0.033	0.60	40.5	0.09	0.46	0.77	3.4	13.7	22.3	1464
SCT 5(Site)															
10/30/02	510	0.50	0.53	0.087	0.068	0.054	1.21	39.8	0.090	0.70	1.22	5.9	13.8	20.4	1394
11/25/02	nn	0.22	0.52	0.095	0.023	0.067	1.32	38.0	0.088	0.80	0.57	6.1	17.9	21.5	2830
01/07/03	468	0.51	0.60	0.121	0.073	0.082	0.92	43.6	0.120	1.16	0.66	5.7	10.9	27.5	542
01/23/03	506	0.47	0.71	0.129	0.041	0.106	1.55	41.2	0.132	1.40	1.24	8.5	12.7	30.0	1541
03/06/03	445	0.98	0.52	0.110	0.051	0.107	nd	44.5	0.139	1.46	0.69	6.5	9.4	23.4	448
04/02/03	293	1.30	0.71	0.134	0.071	0.124	0.86	43.1	0.138	1.26	0.61	6.8	9.0	22.9	179
04/17/03	501	0.86	0.42	0.099	0.048	0.104	0.72	43.6	0.104	0.94	0.85	6.0	4.9	20.0	119
05/13/03	421	0.78	0.40	0.120	0.054	0.092	0.81	42.1	0.121	0.98	0.71	6.1	8.2	20.2	231
06/10/03	662	0.70	0.39	0.105	0.052	0.085	0.71	42.1	0.102	0.87	0.68	5.9	7.1	19.9	312
07/26/03	510	0.58	0.41	0.102	0.045	0.061	0.72	39.2	0.988	7.98	0.65	6.0	7.2	20.2	289

Appendix C

Selective compositions of rain and pore waters (mM) sampled at the SCT 2 and SCT soil sites. Also reported are gravimetric water contents (wt.% in bulk soil).

Date	Na	Mg	K	Ca	Rb	Sr	Cl	Water	Date	Na	Mg	K	Ca	Rb	Sr	Cl	Water
SCT 2 rain									*SCT 5 rain*								
01/06/03	4.1	0.5	0.12	0.23	0.00004	0.0014	4.74	na	01/06/03	5.1	0.6	0.16	0.43	0.00005	0.0018	6.01	na
02/13/03	6.3	0.8	0.2	0.46	0.00007	0.0022	7.56	na	03/06/03	4.6	0.6	0.14	0.40	0.00005	0.0014	5.81	na
04/17/03	4.4	0.6	0.12	0.35	0.00005	0.0013	5.83	na	04/17/03	5.1	0.7	0.12	0.53	0.00004	0.0017	7.05	na
05/01/03	2.9	0.4	0.07	0.19	0.00003	0.0009	3.67	na	05/01/03	1.7	0.2	0.04	0.19	0.00001	0.0008	2.33	na
12/02/03	1.8	0.2	0.1	0.19	0.00002	0.0006	2.76	na	12/02/03	1.7	0.2	0.04	0.15	0.00001	0.0006	1.98	na
12/16/03	3.6	1.2	0.31	0.52	0.00006	0.0027	3.15	na	12/16/03	8.3	1.0	0.22	0.43	0.00006	0.0032	9.85	na
12/31/03	6.2	1.1	0.22	0.31	0.00003	0.0021	2.85	na	12/29/03	4.3	1.7	0.07	0.43	0.00006	0.0035	7.2	na
SCT 2 pore water @ 0.15 m depth									*SCT 5 pore water @ 0.15 m depth*								
11/20/02	855	355	285	1025	0.121	2.98	1410	14.6	03/26/02	237	40	65	116	0.0324	0.301	48	14.9
12/18/02	592	261	247	697	0.100	1.98	993	20.2	04/30/02	224	39	61	118	0.0304	0.305	53	8.2
01/06/03	597	317	230	795	0.093	2.24	1173	21.0	11/25/02	329	166	155	542	0.0778	1.340	609	12.9
01/23/03	429	130	170	344	0.073	0.99	564	18.6	12/13/02	438	224	199	712	0.0967	1.734	925	17.4
02/12/03	516	167	200	444	0.081	1.25	496	17.5	12/18/02	477	269	209	832	0.0983	2.045	1106	17.9
02/27/03	439	129	151	318	0.062	0.90	327	10.2	01/06/03	319	104	139	326	0.0647	0.816	598	25.8
05/01/03	141	28	46	75	0.023	0.23	19	14.0	02/13/03	316	76	116	227	0.0553	0.588	361	16.5
05/13/03	144	35	50	82	0.022	0.27	32	12.4	02/27/03	267	62	100	176	0.0533	0.449	220	13.9
12/02/03	659	290	220	907	0.104	2.78	1315	16.8	04/02/03	224	44	77	122	0.0410	0.322	133	12.1
12/08/03	858	454	269	1324	0.118	3.71	2076	15.2	05/13/03	242	40	77	116	0.0444	0.304	42	12.3
12/16/03	941	541	297	1470	0.123	4.20	2398	16.4	11/18/03	663	369	273	1154	0.1448	3.032	1267	13.8
12/29/03	794	405	258	1200	0.105	3.38	1929	nd	12/02/03	514	216	225	695	0.1479	1.831	1052	15.2
01/06/04	495	151	161	413	0.066	1.20	756	18.1	12/08/03	628	289	236	945	0.1135	2.354	933	17.3
01/13/04	462	102	131	221	0.055	0.69	568	17.2	12/16/03	661	279	223	877	0.0927	2.233	883	13.7
01/21/04	487	102	145	236	0.069	0.74	584	17.8	12/29/03	263	84	124	278	0.0545	0.718	277	16.4
02/10/04	387	68	119	186	0.048	0.53	322	14.1	01/13/04	259	74	115	213	0.0558	0.560	268	18.1
02/27/04	368	69	124	166	0.050	0.55	205	13.4	01/21/04	283	74	106	195	0.0475	0.519	265	18.9
03/24/04	291	31	73	88	0.035	0.26	55	12.4	02/05/04	242	57	99	175	0.0440	0.449	238	17.2
04/08/04	243	24	48	70	0.022	0.20	21	7.2	02/27/04	220	55	101	161	0.0498	0.415	170	nd
SCT 2 pore water @ 1.2 m depth									*SCT 5 pore water @ 1. 2 m depth*								
07/09/02	1086	477	10.9	149	0.005	1.07	643	4.8	06/04/02	489	99	8.0	31.7	0.0096	0.226	429	15.2
11/05/02	800	377	5.3	116	0.003	0.83	429	12.2	12/18/02	538	166	4.7	51.8	0.0053	0.363	463	17.9
11/20/02	876	438	8.9	130	0.005	0.98	519	11.1	01/06/03	511	165	5.4	44.8	0.0039	0.378	587	23.7
01/06/03	619	429	9.1	151	0.004	1.05	638	16.1	02/13/03	424	136	2.6	40.2	0.0028	0.306	485	13.6
02/12/03	590	394	11.4	144	0.006	0.99	643	nd	04/02/03	457	134	2.0	37.5	0.0025	0.284	465	12.2
02/27/03	642	391	10.1	135	0.006	0.92	547	10.0	04/17/03	511	117	2.8	28.8	0.0035	0.248	457	13.4
04/02/03	723	451	8.7	144	0.004	0.99	468	12.3	05/01/03	509	107	4.0	30	0.0047	0.230	437	13.7
04/17/03	597	323	5.5	92	0.002	0.68	135	nd	05/13/03	505	104	4.0	32.2	0.0048	0.239	429	15.1
05/13/03	1270	709	9.2	206	0.004	1.45	53	11.0	12/29/03	537	153	12.2	56.4	0.0104	0.379	578	13.2
11/11/03	2674	325	9.6	148	0.006	1.03	343	10.3	01/06/04	496	207	2.8	59.3	0.0036	0.472	680	7.6
12/29/03	862	428	18.2	191	0.008	1.13	449	14.8	01/13/04	409	185	0.9	52.7	0.0015	0.421	522	8.2
01/06/04	848	631	10.0	229	0.005	1.57	931	11.6	01/21/04	409	183	1.5	55	0.0016	0.426	547	12.6
01/21/04	690	458	16.3	182	0.007	1.27	773	14.2	02/27/04	382	146	2.1	44	0.0018	0.331	488	14.2

(*continued on next page*)

Appendix C (*continued*)

Date	Na	Mg	K	Ca	Rb	Sr	Cl	Water	Date	Na	Mg	K	Ca	Rb	Sr	Cl	Water
02/10/04	513	291	15.3	125	0.006	0.81	488	31.5	03/10/04	381	111	1.5	68.9	0.0014	0.263	276	nd
02/27/04	519	344	14.1	125	0.007	0.90	621	12.1	03/24/04	450	114	4.1	36.8	0.0023	0.260	378	nd
03/24/04	670	361	17.3	146	0.010	0.99	415	nd	04/08/04	438	109	2.4	35.6	0.0026	0.252	384	nd
04/08/04	674	354	16.8	140	0.010	0.93	420	nd	04/19/04	411	98	2.6	29.4	0.0031	0.232	381	nd

may also isolate plants from direct inputs from precipitation and weathering.

The nature of closed versus open system nutrient cycling across the A/B interface is also addressed by quantifying nutrient reservoirs and the reversible and irreversible fluxes between them. The net discharge fluxes for K, Ca and Mg, after subtracting precipitation and weathering, are generally positive indicating that these nutrients are being concentrated in the soils. Although small compared to the amounts of these nutrients cycled through the plants on an annual basis (1–10%), such net nutrient accumulation is not sustainable over the long-term. The plant/soil system appears to be in a state of environmental disequilibrium sustained by the large exchange capacity of the soil. In dynamic coastal ecosystems such as at Santa Cruz, impacts may be related to changes in microclimate and vegetation succession which in the past may have extended the depth of the biotic/abiotic interface.

ACKNOWLEDGEMENTS

Our co-author, colleague and friend Davison Vivit passed away during the writing of this paper and we acknowledge the importance his many contributions to this and other projects over the years. We thank the rangers and staff at Wilder State Park, specifically Tim Hyland, for his help in the field and Stephanie Mills of Laguna Ranch who provided site access on private land for the study. We would like to acknowledge US Geological colleagues and other for helpful discussions and for assistance in the field: Jennifer Harden, Jennie Munster, Carrie Maseillo, Mark Waldrop, Daniel Bain, Suzanne Anderson and Edward Tipper. We thank the two anomalous journal reviewers who provided helpful criticisms and suggestions. Funding was provided by the National Research Program of the Water Resources Discipline of the US Geological Survey.

APPENDIX A

See Appendix Tables A–C.

REFERENCES

Adam D. P., Byrne R. and Luther E. (1981) A late Pleistocene and Holocene pollen record from Laguna de Las Tancas, northern coastal Santa Cruz County, California. *Madrono* **28**, 255–272.

Aniku J. R. E. and Singer M. J. (1990) Pedogenic iron oxide trends in a marine terrace chronosequence. *Soil Sci. Am. J.* **54**, 145–152.

Ashraf M., McNeilly T. and Bradshaw A. D. (1989) The potential for evolution of tolerance to sodium chloride, calcium chloride, magnesium chloride and sea water in four grass species. *New Phytol.* **112**, 245–254.

Barger N. N., D'Antonio C. M., Ghneim T., Brink K. and Cuevas E. (2002) Nutrient limitation to primary productivity in a secondary savannna in Venezuela. *Biotropica* **34**, 493–501.

Beyrouty C. A., West C. P. and Gbur E. E. (1990) Root development and bermuda grass and tall fescue as affected by cutting intervals and growth regulators. *Plant Soil* **127**, 23–30.

Blum J. D., Taliaferro E. H., Weisse M. T. and Holmes R. T. (2000) Changes in Sr/Ca, Ba/Ca and $^{87}Sr/^{86}Sr$ ratios between tropic levels in two forest ecosystems in the northeastern USA. *Biochemistry* **49**, 87–101.

Boudot J. P., Maitat O., Merlet D. and Rouiller J. (1996) Occurence of non-monomeric species of aluminium in unsaturated soils and surface waters: consequences for the determination of mineral saturation indices. *J. Hydrol.* **177**, 867–874.

Brantley S. L. and White A. F. (2009) Approaches to modeling weathered regolith. *Rev. Mineral. Geochem.* **70**, 443–477.

Brantley S. L., White T. S., White A. F., Sparks D., Richter D., Pregitzer K., Derry L. A., Chotover J., Chadwick O. A., April R., Anderson R. S. and Amunson R. (2006) Frontiers in Exploration of the Critical Zone: Report of a workshop sponsored by the National Science Foundation (NSF), October 24–26, 2005, Newark, DE, USA, 35p.

Bullen T. D. and Bailey S. W. (2005) Identifying calcium sources at an acid deposition-impacted spruce forest: a strontium isotope, alkaline earth element multi-tracer approach. *Biogeochemistry* **74**, 63–99.

Bullen T. D. and Eisenhauer A. (2009) Metal stable isotopes in low temperature systems: a primer. *Elements* **5**, 349–352.

Bullen T., White A. F., Blum A., Harden J. and Schulz M. (1997) Chemical weathering of a soil chronosequence on granitoid alluvium: II. Mineralogic and isotopic constraints on the behavior of strontium. *Geochim. Cosmochim. Acta* **61**, 291–306.

Bullen T. D., Fitzpatrick J. A., White A. F., Schulz M. S. and Vivit D. V. (2004) Calcium stable isotope evidence for three soil calcium pools at a granitoid chronosequence. *Water Rock Interact.* **11**, 813–817.

Burnham C. P. (1989) Pedological processes and nutrient supply from parent material in tropical soils. In *Mineral Nutrients in Tropical Forest and Savanna Ecosystems* (ed. J. Proctor). Blackwell Scientific Publication, Oxford, pp. 27–40.

Buss H. L., Bruns M. A., Schulz M. S., Moore J., Mathur C. F. and Brantley S. L. (2005) The coupling of biologic iron cycling and mineral weathering during saprolite formation, Luquillo Mountains, Puerto Rico. *Geobiology* **3**, 247–260.

Cardon Z. G. and Whitbeck J. L. (2007) *The Rhizophere: An Ecological Perspective*. Academic Press, Boston. 378p.

Chadwick O. A., Derry L. A., Vitousek P. M., Huebert B. J. and Hedin B. J. (1999) Changing sources of nutrients during four million years of ecosystem development. *Nature* **568**, 491–497.

Chauduri S., Clauer N. and Semhi K. (2007) Plant decay as a major control of river dissolved potassium: a first estimate. *Chem. Geology* **243**, 178–190.

Christian J. M. and Wilson S. D. (1999) Long-term ecosystem impacts of an introduced grass in the northern Great Plains. *Ecology* **80**, 2397–24072.

Conner J. J. and Shacklette H. T. (1975) Background geochemistry of some rocks, soils, plants and vegetables in the conterminous United States. *US. Geol. Surv. Prof. Paper* **574-F**, 168.

Dasch A. A., Blum J. D., Eagar C., Fahey J., Driscoll C. T. and Siccama T. G. (2006) The relative uptake of Ca and Sr into tree foliage using a whole-watershed calcium addition. *Biogeochemistry* **80**, 21–41.

Ding T. P., Tian S. H., Sun L., Wu L. H., Zhou J. X. and Chen Z. Y. (2008) Silicon isotope fractionation between rice plants and nutient solution and its significance to the study of the silica cycle. *Geochim. Cosmochim. Acta* **72**, 5600–5615.

Driscoll C. T., van Breemen N. and Mulder J. (1985) Aluminium chemistry in a forested spodosol. *Soil Sci. Soc. Am. J.* **49**, 437–444.

Driscoll C. T., Fallon-Lambert K. and Chen L. (2005) Acidic deposition: sources and effects. In *Encyclopedia of Hydrological Sciences* (ed. M. G. Anderson). John Wiley and Sons, New York, pp. 264–289.

Drobner U. and Tayler T. (1998) Conditions controlling relative uptake of potassium and rubidium by plants from soils. *Plant Soil* **201**, 285–293.

Duke J. A. (1997) *The Green Pharmacy*. Rodal Press, Los Angeles. 452pp.

Faure G. and Mensing T. (2005) *Isotopes: Principals and Applications*. John Wiley & Sons, Holbaken, 367pp.

Fraysse F., Pokrovsky O. S. and Meunier J. D. (2010) Experimental study of terrestrial plant litter interaction with aqueous solutions. *Geochim. Cosmochim. Acta* **74**, 70–84.

Galy A., Yoffe O., Janney P., Williams R., Cloquet C., Alard O., Haliez L., Wadhwa M., Hutcheon I. D., Ramon E. and Carignan J. (2003) Magnesium isotope heterogeneity of the isotope standard SRM980 and new reference materials for magnesium isotope ratio measurements. *J. Anal. At. Spectrom.* **18**, 1352–1356.

Gibson D. J. (2009) *Grasses and Grassland Ecology*. Oxford University Press, Oxford, 435pp.

Giron H. C. (1973) Comparison of dry ashing and wet digestion in the preparation of plant material for atomic absorption analysis. *At. Absorpt. Newsletter* **12**, 28–30.

Gregory P. J. (2006) *Plant Roots, Growth, Activity and Interaction with Soils*. Blackwell Publishing, Ames, 445pp.

Handi H., Eil-Samie A. G. and Ghazy H. (1988) Planting and grow characteristic of flax in saline environments. *Egypt. J. Soil Sci.* **23**, 451–463.

Heister-White J. L., Knapp A. K. and Kelly E. F. (2008) Increasing precipitation events and increases in above-ground net primary productivity in a semi-arid grassland. *Oecologia* **158**, 12–140.

Henry H. A. L., Brizgys K. and Field C. B. (2008) Litter decomposition in a California annual grassland: interactions between photodegradation and litter layer thickness. *Ecosystems* **11**, 545–554.

Huntington T. G. (2000) The potential for calcium depletion in forest ecosystems of the southeastern United States: review and analysis. *Glob. Biogeochem. Cycles* **14**, 623–638.

Jobbagy E. G. and Jackson R. B. (2001) The distribution of soil nutrients with depth: global patterns and the imprints of plants. *Biogeochemistry* **51–77**, 51–77.

Kabata-Pendias A. and Pendias H. (2001) *Trace Elements in Soils and Plants*. CRC Press, Boca Raton, 534 pp.

Kelly E., Chadwick O. A. and Hilinski T. A. (1998) The effect of plants on minerals weathering. *Biogeochemistry* **42**, 21–53.

Maathius F. J. (2009) Physiological functions of mineral macronutrients. *Curr. Opin. Plant Biol.* **12**, 250–258.

Maher K., Steefel C. I. and White A. F. (2009) The role of reaction affinity and secondary minerals in regulating chemical weathering rates at the Santa Cruz marine terrace chronosequence, California. *Geochim. Cosmochim. Acta* **73**, 2804–2831.

Marcum K. B. (20010 Growth and physiological adaptations of grasses to salinity stress. In *Handbook of Plant and Crop Physiology* (ed. M. Pessarakli). CRC Press, Raton Rouge. 478pp.

Marschner H. (1995) *Mineral Nutrition of Higher Plants*. Academic Press, London, 635 pp.

Monaco T. A., Johnson D. A., Norton J. M., Jones T. A., Connors K. J., Norton J. B. and Redinbaugh M. B. (2003) Contrasting responses of Intermountain West grasses to soil nitrogen. *J. Range Manage.* **56**, 282–290.

Moore J., Macalady J. L., Schulz M. S., White A. F. and Brantley S. L. (2009) Shifting microbial community structure across a marine terrace grassland chronosequence, Santa Cruz, Californina. *Soil Biol. Biochem.* **42**, 21–31.

Murphy J., Mead D. and Zaur E. A. (1994) Shoot and root growth response of perennial ryegrass to fertilizer placement depth. *Agron. J.* **86**, 828–832.

Page B. D., Bullen T. D. and Mitchell M. J. (2008) Influences of calcium availability and tree species on Ca isotope fractionation in soil and vegetation. *Biogeochemistry* **88**, 1–13.

Peltola P., Brun C., Astom M. and Tomilina O. (2008) High K/Rb ratios in stream waters – Exploring plant litter decay, groundwater and lithology as a potential controlling mechanism. *Chem. Geol.* **257**, 92–100.

Perez C. A. and Franci J. L. (2007) Macronutrient cycling in mountain grasslands of Sierra de la Ventana, Argentina. *Ecologia Australia* **17**, 199–216.

Perg L. A., Anderson R. S. and Finkel R. C. (2001) Use of a new ^{10}Be and ^{26}Al inventory method to date marine terraces, Santa Cruz, California, USA. *Geology* **29**, 879–882.

Phillips J. D. (2007) Development of textual contrasts in soils by a combination of bioturbation and translocation. *Catena* **70**, 92–104.

Pinney C., Aniku J., Burke R., Harden J., Singer M. J. and Munster J. (2002) Soil chemistry and mineralogy of the Santa Cruz terraces. *U.S. Geo. Surv. Open File Rept.* **02–277**, 10p.

Poszwa A., Dambrine E., Ollier B. and Atteia O. (2000) A comparsion between Ca and Sr in a forested ecosystem. *Plant Soil* **225**, 299–310.

Richter D. D. and Markewitz M. D. (1995) How deep is soil? *Bioscience* **45**, 600–608.

Schmidt A., Stille P. and Vennemann T. (2003) Variations of the ^{44}Ca/^{40}Ca ratio in seawater during the past 24 million years: evidence from δ^{44}Ca and δ^{18}O values of Miocene phosphates. *Geochim. Cosmochim. Acta* **67**, 2607–2614.

Scurlock J. M. O., Johnson K. and Olson R. J. (2002) Estimating net primary productivity from grassland biomass dynamic measurements. *Global Change Biol.* **8**, 736–753.

Shaffer J. A., Jung G. A. and Narem U. R. (1994) Root and shoot characteristics of prairie grass compared to tall fescue and smooth brome grass during establishment. *New Zeal. J. Agr. Res.* **37**, 143–151.

Schulz M. S., Vivit D. V., Schulz C., Fitzpatrick J. and White A. F. (2010) Biologic origin of iron nodules in a marine terrace chronosequence, Santa Cruz California. *Soil Sci. Am. J.* **74**, 550–564.

Smit A. M., Kooijman A. M. and Sevink J. (2002) Impact of grazing on litter decomposition and nutrient availability in a grass-encroached Scott pine forest. *For. Ecol. Manag.* **158**, 117–126.

Snyman H. A. (2009) Root studies on grass species in a semi-arid South Africa along a degradation gradient. *Agric. Ecosyst. Environ.* **130**, 100–108.

Stone L. E. and Kalisz P. J. (1991) On the maximum extent of tree roots. *For. Ecol. Manag.* **46**, 59–102.

Stonestrom D. A., White A. F. and Akstin K. C. (1998) Determining rates of chemical weathering in soils-solute transport versus profile evolution. *J. Hydrol.* **209**, 331–345.

Stromberg M. R., Corbin J. D. and D'Antonio C. M. (2007) *California Grasslands*. University of California Press, Berkeley, 467pp.

Thill D. C., Beck K. G. and Callihan R. H. (1984) The biology of Downy Brome (*Bromus tectorum*). *Weed Sci.* **32**, 7–12.

Tipper E. T., Gallardet J., Louvat P., Capmas F. and White A. F. (2010) Mg isotope constraints on soil pore-fliud chemistry: evidence from Santa Cruz, California. *Geochim. Cosmochim. Acta* **74**, 3883–3896.

Trudgill S. T. (1988) *Soil and Vegetation Systems*. Claredon Press, Oxford, 398pp.

Tyler G. (2004) Ionic charge, radius and potential control root/soil concentration ratios of fifty catonic elements in the organic horizon of a beech (*Fagus sylatica*) forest podsol. *Sci. Total Environ.* **329**, 231–239.

Velbel M. A. (1995) Interaction of ecosystem processes and weathering processes. In *Solute Modelling in Catchment Systems* (ed. S. T. Trudgill). John Wiley & Sons Ltd., London, pp. 327–367.

Velde B. and Barré P. (2010) *Soils, Plants and Clay Minerals*. Springer-Verlag, Berlin, 428pp.

Veresoglou D. S., Barbayiannis N., Matsi T., Anagnostopoulos C. and Zalidis G. C. (1996) Shoot Sr concentrations in relation to shoot Ca concentrations and to soil properties. *Plant Soil* **178**, 95–100.

Whipkey C. E., Capo R. C., Chadwick O. A. and Steward B. W. (2000) The importance of sea spray to the cation budget of a coastal Hawaiian soil: a strontium isotope approach. *Chem. Geol.* **168**, 37–48.

White A. F., Schulz M. S., Vivit D. V., Blum A. E., Stonestrom D. A. and Anderson S. P. (2008a) Chemical weathering of a marine terrace chronosequence, Santa Cruz, California I: interpreting rates and controls based on soil concentration-depth profiles. *Geochim. Cosmochim. Acta* **72**, 36–68.

White A. F., Bullen T. B., Vivit D. V. and Schulz C. (2008b) Chemical interactions in rainfall/shallow pore waters in coastal watersheds. *Geochim. Cosmochim. Acta* **72**, A1017.

White A. F., Schulz M. S., Stonestrom D. A., Vivit D. V., Fitzpatrick J., Bullen T. D., Maher K. and Blum A. E. (2009) Chemical Weathering of a marine terrace chronosequence, Santa Cruz California. Part II: solute profiles, gradients and the comparison of short and long-term weathering rates. *Geochim. Cosmochim. Acta* **73**, 2769–2803.

Whitehead D. C. (2000) *Nutrient Elements in Grasslands Soil–Plant–Animal Relationships*. CABI Publishing, Wallingford, 345pp.

Wyttenbach A., Furrer V. and Tobler L. (1995) The concentration ratios plant to soil for the stable elements Cs, Rb and K. *Sci. Total Environ.* **173–174**, 361–367.

Associate editor: Donald L. Sparks